

## Article

# Multi-Model Assessment of Streamflow Simulations under Climate and Anthropogenic Changes Exemplified in Two Indian River Basins

Anusha Somisetty <sup>1,†</sup> , Akshay Pachore <sup>1,†</sup>, Renji Remesan <sup>1,\*</sup>  and Rohini Kumar <sup>2,\*</sup> 

<sup>1</sup> School of Water Resources, Indian Institute of Technology Kharagpur, Kharagpur 721302, India; anu.somisetty11896@gmail.com (A.S.); abpachore@gmail.com (A.P.)

<sup>2</sup> UFZ-Helmholtz Centre for Environmental Research GmbH, Permoserstraße 15, 04318 Leipzig, Germany

\* Correspondence: renji.remesan@swr.iitkgp.ac.in (R.R.); rohini.kumar@ufz.de (R.K.)

† These authors contributed equally to this work.

**Abstract:** This study aims to evaluate the climate- and human-induced impacts on two contrasting river basins in India, specifically, the Ganges and the Godavari. Monthly discharge simulations from global hydrological models (GHMs), run with and without human influence using CMIP5 projections under the framework of the Inter-Sectoral Impact Model Intercomparison Project, are utilized to address the scientific questions related to the quantification of the future impacts of climate change and the historical impacts of human activities on these river basins. The five state-of-the-art GHMs were considered and subsequently used to evaluate the human and climate change impacts on river discharges (seasonal mean discharge and extreme flows) during the pre-monsoon, monsoon, and post-monsoon seasons under the RCP2.6 and RCP8.5 emission scenarios. Results showed that human impacts during the baseline period on long-term seasonal discharge in the Ganges and Godavari River basins for the pre-monsoon season are around 40% and 23%, respectively, and these impacts are stronger than the future climate change impact in the pre-monsoon season for the Ganges basin, whereas, for the Godavari basin, the same pattern is observed with some exceptions. The human impact in the course of the historical period on the pre-monsoon flows of both the Ganges and the Godavari are more significant than on the monsoon and post-monsoon flows. In the near future (2010–39) time slice, the impact of climate change on the streamflow of the Ganges is highest for the post-monsoon season (13.4%) under RCP 8.5 as compared to other seasons. For Godavari, in the near-future period, this impact is highest for the pre-monsoon season (18.2%) under RCP 2.6. Climate-induced changes in both of the basins during both the monsoon and post-monsoon seasons is observed to have a higher impact on future flows than direct human impact-induced changes to flow during the current period. High flows (31.4% and 19.9%) and low flows (51.2% and 36.8%) gain greater influence due to anthropogenic actions in the time of the pre-monsoon season compared to other times of year for the Ganges and Godavari basins, respectively. High flows for the Ganges during the near future time slice are most affected in the monsoon season (15.8%) under RCP 8.5 and, in the case of the Godavari, in the pre-monsoon season (18.4%) under the RCP 2.6 scenario. Low flows of the Ganges during the near-future period are most affected during the monsoon season (22.3%) and for the Godavari, low flows are affected most for the post-monsoon season (22.1%) under RCP 2.6. Uncertainty in the streamflow estimates is more pronounced for the Godavari basin compared to the Ganges basin. The findings of this study enhance our understanding of the natural and human-influenced flow regimes in these river basins, which helps the formation of future strategies, especially for inter-state and transboundary river management.

**Keywords:** Ganges; Godavari; human impact; climate change; GHM; CMIP5; ISIMIP



**Citation:** Somisetty, A.; Pachore, A.; Remesan, R.; Kumar, R. Multi-Model Assessment of Streamflow Simulations under Climate and Anthropogenic Changes Exemplified in Two Indian River Basins. *Water* **2022**, *14*, 194. <https://doi.org/10.3390/w14020194>

Academic Editor: Aizhong Ye

Received: 18 November 2021

Accepted: 7 January 2022

Published: 11 January 2022

**Publisher's Note:** MDPI stays neutral with regard to jurisdictional claims in published maps and institutional affiliations.



**Copyright:** © 2022 by the authors. Licensee MDPI, Basel, Switzerland. This article is an open access article distributed under the terms and conditions of the Creative Commons Attribution (CC BY) license (<https://creativecommons.org/licenses/by/4.0/>).

## 1. Introduction

Human activities along with climate change play a crucial role in the future changes to hydrological circulation around the globe. In recent years, there have been global efforts to study the relationships between climate change and human activities and their influence as the main drivers of streamflow changes in river basins [1]. The effect of climate change and human activities together is referred to as environmental change, and this has a direct influence on streamflow [2] and an indirect influence on drought [3]. Human activities, including water abstraction for irrigation and drinking water supply, hydropower generation, water use for industrial purposes, reservoir and dam operations, and other human influences in the form of urbanization, agricultural practices, the construction and operation of hydraulic structures, etc., influence monsoon peak flows and impact pre-monsoon low flows [4].

To study the regional and river basin-scale differences and associated uncertainties in a comprehensive way, the multi-model comparison approach is essential for employing human impact parameterizations in combination with hydrological models under different scenarios [5]. The Inter-Sectoral Impact Model Intercomparison Project (ISIMIP; [www.isimip.org/](http://www.isimip.org/); accessed on 20 May 2019 [6]) is a good example of such a framework, given that it focuses on the consistent evaluation of impact models with respect to the representation of extreme events across various sectors [6,7]. Under this framework, multiple state-of-the-art global hydrological models (GHMs) are joined with coupled model intercomparison project phase 5 (CMIP5) projections taken from bias-corrected global climate models and representative concentration pathways (RCPs) to obtain hydrologic simulations under natural and human-influenced conditions. So far, ISIMIP simulations have been widely used by many researchers studying water resources to evaluate the impacts of climate change and human water management on flow regimes and droughts [6,8–11].

Though there are differences in process simulation, global hydrological models (GHMs) are useful tools for evaluating the future flood and drought trend predictions under natural and human-influenced settings. GHMs estimate sectoral water demands by using a combination of socioeconomic and hydro-climatological parameters [12,13]. Researchers [14] have used the PCR-GLOBWB model to assess groundwater depletion on a global scale. Another detailed study [15] used an extended version of the VIC model proposed in a previous study [16] to model runoff and discharge at the global scale. Researchers [17] have also attempted to demonstrate the application of a state-of-the-art global hydrological model (H08) to estimate the global virtual water flow. Another subsequent study [18] has enhanced the water abstraction schemes of the H08 model and their application at regional to global scales.

Sea level rise due to climate change and human activities exerts pressure on the coastal ecosystems, such as mangroves, from both the seaward side and landward side in the Godavari basin [19]. Studies indicating that a warmer climate is observed in a few sub-basins of the Godavari show that if this warmer climate leads to water shortage in the basin, the water-sharing agreements in the basin will be affected [20]. Due to different hydro-climatic, social, and environmental conditions, researchers must study the current effects on and future changes to the availability of freshwater resources for agricultural, industrial, recreational, and social needs in these nationally relevant Indian river basins.

Though global scale studies have highlighted the strong impacts of human activities on river discharge in Indian river basins, less understood is how the Ganges and Godavari compare and contrast with each other in terms of human vs. climate change impacts. A study [21] reported that surface water and groundwater losses were high in the Ganges basin because of intensive irrigation. Another study suggested that human water use has a considerable impact on the terrestrial water storage of the Ganges basin [13]. One recent study shows that the combined impacts of climate change and anthropogenic activities affects the sustainability of the Ganges–Brahmaputra–Meghna delta and highlighted the river basin's importance for the social and environmental sustainability dynamics of the region [22]. Some researchers have highlighted that the incorporation of human impact

parameterizations in GHMs results in improved estimates of monthly discharges and hydrological extremes [10]. A quantitative combined assessment of the impact of human activities along with climate change, with the help of the ISIMIP-based impact model simulations, would help to inform about the possible management strategies of water resources in these river basins, and may provide guidelines to subsequent adaptation measures.

This study attempts to incorporate GHMs with and without human impact parameterizations under contemporary and future climate projection scenarios to assess the impact of climate variation and human water management on seasonal mean discharges and extreme flows in the Ganges and Godavari River basins. To fulfill the aim of the study, the following objectives are formulated: (i) quantify the relative contribution of impacts due to human activities and climate change on seasonal discharge, and investigate the more prominent impact in the two river basins; (ii) evaluate the contributions of climate change and human activities to streamflow variability across seasonal timescales (pre-monsoon, core monsoon, and post-monsoon); and (iii) assess and contrast the impact of human activities and climate change on seasonal high flows ( $Q_{10}$ ) and low flows ( $Q_{90}$ ) to evaluate their relative contribution. To accomplish these objectives, we have analyzed a set of streamflow simulations from GHMs in combination with five bias-corrected, downscaled climate model projections (CMIP5) for RCP 2.6 and RCP 8.5 scenarios.

## 2. Materials and Methods

### 2.1. Study Area Details

(A) Ganges Basin: The Ganga (Ganges) rises from the Gangotri Glacier in the Himalayas (Figure 1). The extent of the basin is  $73^{\circ}2'$  to  $89^{\circ}5'$  E and  $21^{\circ}6'$  to  $31^{\circ}21'$  N. The population in the basin is 329.16 M. The total drainage area of the basin is 1,086,000 km<sup>2</sup>. A large part of the basin area lies in India (862,769 km<sup>2</sup>), followed by Nepal, Bangladesh, and China. The Ganges and its tributaries flow through 11 states of India. The elevation of the basin ranges from 8000 m to 0 m (near the coast). The annual rainfall varies between 400 mm and 2000 mm. Most of the rainfall occurs during the monsoon months, i.e., June to October. There are 144 major and 334 medium-sized irrigation projects, 39 hydroelectric projects, and 56 powerhouses in the basin. The Ganges river basin is mainly covered with agriculture (66%) and forest area (16%), as depicted using the land use and land cover map [23] in Figure 1. The total water resource potential is 525.02 BCM, out of which 250.0 BCM is utilizable surface water potential in Ganges river basin [24].

(B) Godavari Basin: The Godavari is the largest river in the Indian peninsular region and the second largest river basin in India (Figure 1). The Godavari basin covers 10% of the geographical area of the country (Figure 1). It covers an area of 312,812 km<sup>2</sup> [25], out of which 48.7% falls in Maharashtra, 23.7% in Andhra Pradesh, followed by Chhattisgarh, Madhya Pradesh, Odisha, Karnataka, and the Union Territory of Puducherry. The Godavari basin lies in the Deccan plateau with an extent between  $73^{\circ}24'$  and  $83^{\circ}4'$  E and  $16^{\circ}19'$  to  $22^{\circ}34'$  N. The annual rainfall varies from 755 mm to 1531 mm and the average annual rainfall (1971–2005) is 1097 mm, out of which 84% of annual rainfall is obtained during the monsoon season [20]. In the case of land cover and land use, 59.57% of the basin area is covered with agricultural land, 29.78% is covered with forest, and 2.06% of the basin area is occupied by water bodies (Figure 1). There are 70 major and 216 medium-sized irrigation projects, and 14 hydro-electric projects in the basin. The total annual water potential is 110.54 BCM, out of which the utilizable surface water is 76.30 BCM [26].

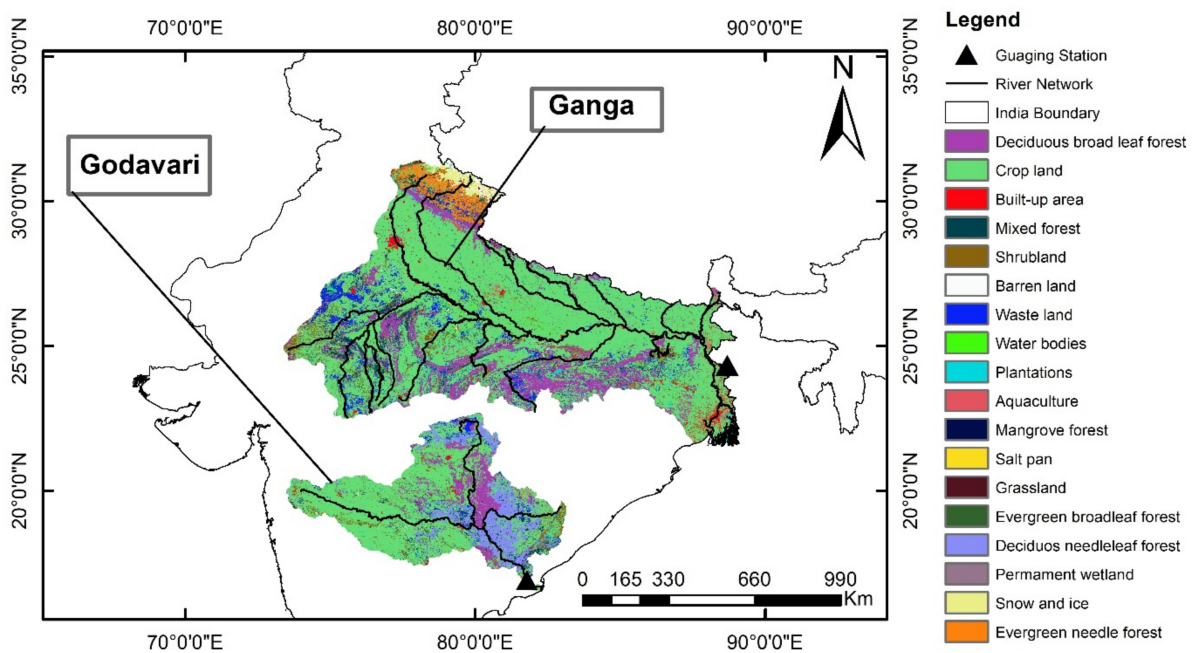


**Figure 1.** Study area location (the Ganges and Godavari basins) in India, overlaid upon dominant land cover/uses.

A recent study [8] found that human activities resulted in the reduction of low flows in Asia. In these regions, peculiar hydrological scenarios, such as (i) the impact of reservoir operations being exceeded by water abstraction and (ii) extensive water withdrawals leaving the rivers dried up in the pre-monsoon season, etc., are observed in certain river basins. India as a country, though generally characterized by abundant water resources due to the distributed nature of its monsoon and its larger river networks, is going through tremendous hydrological and ecological stresses with regard to its river basins. India’s water consumption is high in the agriculture sector (89% for irrigation) as compared to the other sectors (7% for domestic and 4% for industrial purposes) [27]. India [28] also has the second highest irrigated land area, which is about 70 Mha [29]. However, this study focuses only on the above-mentioned two contrasting river basins of India, specifically, the Ganges and the Godavari, with different socio-environmental and agro-climatological settings. The Ganges is the largest river basin and the Godavari is the second largest river basin in India, with distinct hydrological challenges. These river basins provide water for drinking, irrigation, hydropower generation, and industrial, navigational, and recreational purposes. Agriculture accounts for 66% of the Ganges basin [24] area and 60% of the Godavari basin [26] area. The specific details of the selected river basins are given in the Table 1.

**Table 1.** Main features of the Ganges and Godavari basins [24,26].

Features	Ganges Basin	Godavari Basin
Extent of the basin	73°2' to 89°5' E and 21°6' to 31°21' N	73°24' to 83°4' E and 16°19' to 22°34' N
Population served in millions	329.16	60.49
Drainage area (km <sup>2</sup> )	1,086,000	312,812
Elevation (m)	8000–0	2100–300
Annual rainfall (mm)	400–2000	755–1531

Table 1. Cont.

Features	Ganges Basin	Godavari Basin
Projects	144 major irrigation projects 334 medium-sized irrigation projects 39 hydro-electric projects 56 powerhouses	70 major irrigation projects 216 medium-sized irrigation projects 14 hydro-electric projects
Agriculture area (%)	66	59.57
Forest area (%)	16	29.78
Total water resource potential in BCM (billion cubic meters)	525.02	110.54
Utilizable surface water potential in BCM	250.000	75.30

## 2.2. Hydro-Climatic Datasets

The ISIMIP is an initiative for projecting climate change impacts across different sectors. Five state-of-the-art GHMs, namely, H08 [17,30–32], MPI-HM [33], PCR-GLOBWB [12,34,35], VIC [15,36,37], and WaterGAP2 [21,38–47], are considered in the study. The ISIMIP is a community-driven project wherein global hydrologic simulations are conducted following a protocol established within the global water sector. The GHM simulations considered here refer to ISIMIP fast track runs [6], wherein a set of climate (Representative Concentration Pathways; RCPs) and socio-economic (Shared Socio-economic Pathways; SSPs) inputs were used to drive a set of GHMs. These GHM simulations help to study the implications of changes to water resources and flooding, and the impacts of these on other related sectors [6,8,10,11]. Here, we analyze monthly discharge simulations from above five GHMs, which were combined with CMIP5 projections taken from five GCMs under two RCPs (the low warming scenario, RCP 2.6, and the highest warming scenario, RCP 8.5). The five GCMs considered are GFDL-ESM2M, HadGEM2-ES, IPSL-CM5A-LR, MIROC-ESM-CHEM, and NorESM1-M. The outputs of the climate models are bias corrected and downscaled, before being combined with the hydrologic models within the ISIMIP protocol, using a trend preserving approach [48]. The GHMs were selected based on data availability and a consideration of the hydrological processes, and specifically streamflow simulations, under human intervention activities (e.g., irrigation, reservoir and dam operations, etc.). A representation of the main processes accounted for within the selected GHMs, and other details, are given in Table 2. Readers interested in more details on these datasets may refer to the ISIMIP ([www.isimip.org](http://www.isimip.org), access on 18 November 2021). External users who are not participants of the ISIMIP can request access to the GHM simulations via the ISIMIP website (<https://www.isimip.org/gettingstarted/data-access/>; accessed on 20 May 2019), along with the runs that are available from the worldwide large river basin application work based on the ISIMIP [49].

The monthly simulated discharges for this study are based on the ISIMIP (fast track version). Gridded fields of monthly routed discharge from the ISIMIP were available at 0.5-degree spatial resolutions for the period 1971–2099, with a historical period ranging between 1950 and 2005 and future simulations under different RCPs from 2006 to 2099. As a community project, different modelling groups established their GHMs for the ISIMIP-related simulations. In many cases, the underlying model parameterizations were constrained using the global runoff data base of Global Runoff Data Centre (GRDC, BAFG, Germany) and driven by observed climate forcings. The latter varied depending on the model configuration and the modeler’s prior experience (e.g., CRU, GPCC, WATCH forcing datasets). Details of each selected GHM settings and characteristics are provided on the ISIMIP webpage (fast track version; <https://www.isimip.org/impactmodels/> accessed on 15 May 2019). Since our study relies on these (external) hydrologic simulation databases that were pre-compiled, we analyzed the consistency and plausibility of GHM streamflow simulations to study the river basins, and contrasted the modelled discharge with other

observations. For this, we obtained observed monthly discharge ( $\text{m}^3/\text{s}$ ) data for a location (Farakka) close to the outlet of the Ganges basin for the period 1961–1973 from the GRDC database. The observed monthly discharge ( $\text{m}^3/\text{s}$ ) data for a location (Polavaram) close to the outlet of the Godavari basin from 1971 to 2000 was taken from the India-WRIS website (<https://indiawris.gov.in/wris/> accessed on 6 November 2019).

### 2.3. Methodology

The basis of the study is an attempt to understand the effect of climate and human factors on streamflow, which can be quantified in relative terms based on the comparison of results from two different data slices. The study has considered the ISIMIP simulations that make use of two socio-economic scenario runs: one is with the enabling of the human impact parametrizations (HIPs) in all models, and this simulation run is known as the pressoc scenario; another one is without enabling the HIPs, and is known as nosoc. In the nosoc GHM simulations, the HIPs are switched OFF, which means the model simulations involve (i) a naturalized flow condition, (ii) no human influences, except for year 2000 constant land-use patterns, (iii) no anthropogenic water abstraction (e.g., irrigation), (iv) no consideration of reservoirs/dams, and (v) no population and GDP data prescribed. In the case of pressoc simulations, the GHM runs are with HIP simulations switched ON. That means that the model simulations (i) are with consideration of present-day human impact runs (only the climate varies), (ii) keep all other settings (population, GDP, land use, technological progress, etc.) constant at year 2000 values, (iii) maintain the adaptation pressure under current socioeconomic conditions, and (iv) include present-day irrigation and other water uses/reservoirs. From the baseline and future discharge simulations of pressoc and nosoc, we estimated the climate change impact in the future and the human-induced impact on historical periods, as discussed below.

The detailed methodology adopted in this study is given in Figure 2. The historical period considered here is 1971–2000. The future simulation period under consideration is 2010–99 and it has been divided into 30-year time slices, namely, 2010–39, 2040–69, and 2070–99. For each GCM–GHM–RCP–nosoc/pressoc scenario, the three-month moving average of monthly discharge for the historical as well as the future period was calculated. Then, 30-year long-term seasonal means were calculated for the pre-monsoon season (MAM: Mar–Apr–May), the core monsoon season (JAS: Jul–Aug–Sep), and the post-monsoon season (OND: Oct–Nov–Dec) [50]. The choice of these months was made (i) based on the prominence of progress and the retreating of the monsoon in these river basins, (ii) to maintain the uniformity in the analysis, and (iii) to avoid biasness in moving average due to different time lengths. We, then, computed the contributions of human activities and climate change on streamflow using the long-term seasonal means, as follows:

$$\text{Climate change impact in future period} = \frac{\text{future nosoc} - \text{histnosoc}}{\text{histnosoc}} \times 100 \quad (1)$$

$$\text{Human – induced impact in historical period} = \frac{\text{histpressoc} - \text{histnosoc}}{\text{histnosoc}} \times 100 \quad (2)$$

where, *histnosoc* and *histpressoc* are the simulated outputs corresponding to the historical period considered (1971–2000) for the nosoc and pressoc scenarios, respectively. The *future nosoc* refers to the nosoc simulations corresponding to future periods, i.e., the 30-year time slices of 2010–39, 2040–69, and 2070–99.

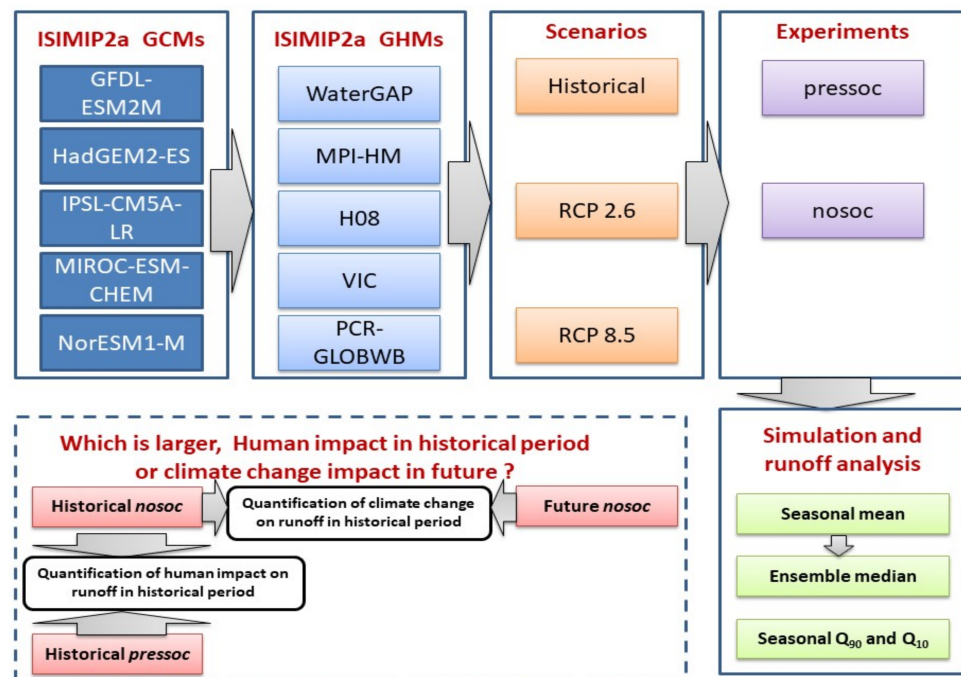


**Figure 2.** Flow chart depicting the main methodology adopted in this study.

As the distributions of the data from different GCM–GHM model combinations are skewed, the mean of the relative change values may be affected by the outliers. Therefore, here, we computed the ensemble median of the relative changes over the 25 combinations of GCMs–GHMs ( $5 \times 5$ ) for a given RCP and time-slice window. Previous studies [50] (for example, Almazroui et al. (2020)) also considered the ensemble median of CMIP6 models to estimate the annual mean temperature and subsequent impact studies. Further, the Taylor diagram is used for selecting GCM–GHM combinations that show good agreement with the observed monthly mean streamflow values. The Taylor diagram consists of the RMSE of the simulated data of the model, the standard deviation of the model and the observed data, and the correlation coefficient of the model data with the observed data. The selected best three ensemble model combinations are the ones with a higher correlation coefficient, a lower RMSE, and a standard deviation closer to standard deviation of the observed streamflow data. The ensemble median of the best selected combinations is also calculated for further different seasonal comparisons. Note that the human-induced changes mentioned in this study are represented only for the historical period during which all GHMs consider the contemporary human intervention impacts [6,39]. During the future climate projection periods, the human intervention activities are kept at the level of the contemporary period [8,10,39]. Furthermore, the climate change impacts are considered for the natural flows in the “nosoc” simulations, while the “pressoc” conditions are set to contemporary levels. These experiments were established with the goal of contrasting the future climate change-induced streamflow projections with the corresponding (streamflow) changes caused by contemporary human interventions. In this way, we want to analyze the level and time period at which climate change-induced streamflow changes contrast with those of the current human-induced changes across the two large-scale Indian river systems. In these experiments, apart from the seasonal mean streamflow changes, we also analyze the projected changes in extreme streamflow conditions (see Figure 2 for the methodological flow chart). To this end, we estimated the 10th and 90th percentile of the seasonal flows characterizing the dry and wet streamflow states for each GCM–GHM–RCP combination for the historical as well as the 30-year projected time slices. We then calculated the relative change in the long-term seasonal discharges (extreme flows) and then summarized the projected changes in the (seasonal) streamflow extremes as an ensemble median alongside the variability, which were computed based on different

model combinations for the considered emission scenarios (RCP 2.6 and RCP 8.5). The ensemble median values of relative changes in extreme streamflow are also calculated for the best selected GCH–GHM model combinations for comparison. In this study, we have used a simple approach to calculate the ensemble mean and median to take care of the model uncertainty by converting the timeseries data into monthly averaged data and then stacking data from all 25 models one below another and taking the arithmetic average to obtain monthly mean values of this ensemble dataset from the 25 model (5GCH\*5GHM) combinations.

**Table 2.** Main features of considered hydrological processes and human factors in selected GHMs [14–16,51,52].

Hydrological Process	Global Hydrological Models [12,13,17,18]				
	H08	MPI-HM	PCR-GLOBWB	VIC	WaterGAP2
Potential evapo-transpiration scheme	Bulk formula	Penman–Monteith	Hamon	Penman–Monteith	Priestley–Taylor
Snowmelt scheme	Energy balance	Degree day	Degree day	Energy balance	Degree day
Surface runoff scheme	Saturation excess	Saturation excess	Saturation excess	Saturation excess	Saturation excess
River routing scheme	Based on 30 m drainage direction map	Linear reservoir cascade	Travel time routing	Linear reservoir cascade	Linear reservoir cascade
Human factors considered	Agriculture, household use, business, and desalination	Agriculture sector	Agriculture, household, livestock, and business.	Not included	Agriculture, domestic, livestock, production, and business

Previous studies [21,35] reported that the human impact is always negative, which means that the impact of dam and reservoir operations and return flows is exceeded by water abstraction. The impact of climate change is sometimes positive, which means that climate change increases the flows, and sometimes it is negative [35,53]. The main reason for increased flow due to climate change is connected with the potential increase in snow melt volume in the Ganges basin due to warming temperatures and changes to the monsoon dynamics. As reported in previous studies, this increase is also governed by “enhanced thermodynamic conditions due to atmospheric warming” [50,54]. If the average of the relative change values of the future “nosoc” scenario with respect to historical “nosoc” is taken, it may result in zero, indicating that climate change has no effect on discharge and, thus, will lead to false conclusions. To avoid this, the absolute values of the relative change are considered and the median of the absolute relative changes for the 30-year time slices, i.e., 1971–2000 (historical period), 2010–39 (near future), 2040–69 (mid-future), and 2070–99 (far future), was calculated to quantify the impacts of climate change and human activities on seasonal mean discharges. Similarly, in this study, we considered the Q90 and Q10 as per the National River Flow Archive’s flow statistics derived by the UK Centre of Ecology and Hydrology. Here, the Q10 (the 90th percentile flow) is the flow in cubic meters per months that was equaled or exceeded for 10% of the considered flow data—it is a high flow indicator. Q90 (the 10th percentile flow) denotes the flow in cubic meters per month that was equaled or exceeded for 90% of the flow record. The Q90 flow is an indicator of low-flow behavior.

### 3. Results

Based on the methodology described above (see also Figure 2), the human-induced effect for the historical period of 1971–2000 (historical-nosoc vs. historical-pressoc) and climate change (historical-nosoc vs. future-nosoc) effect for the future period 2010–99 under RCP 2.6 and RCP 8.5 are evaluated in this section. By contrasting these two sets of GHM

simulations across the two large Indian river basins, the level at which the climate-induced changes in the future dominate the contemporary level of human impact, or vice versa, can be inferred.

Before moving forward with any analysis, it is crucial to know how close the observed river flow is with the simulated streamflow from the 25 GCM–GHM combinations of the Ganges and Godavari river basins during the overlapping baseline periods. Thus, we began our analysis by comparing the India-WRIS and GRDC’s observational streamflow data with those of the GHMs simulated flow at monthly temporal resolutions. As these GHM runs are driven using climate model projections, though they are bias corrected, we do not expect to catch the exact observed temporal dynamics (e.g., month-to-month variability). To obtain the best match with the observed data, we have selected the three best-performing GCM–GHM ensemble combinations based on the Taylor diagram. Figure 3 shows the Taylor diagrams with three different parameters, i.e., the RMSE (green dotted lines), the standard deviation of the model data (black dotted lines), the standard deviation of the observed data (red line), and the correlation coefficient (blue dotted lines). The best three member GCM–GHM ensemble combinations for the Ganges are (WaterGAP-NorESM1-M), (WaterGAP-MIROC-ESM-Chem), and (WaterGAP-HADGEM2-ES), and for the Godavari River, the corresponding ensemble combinations are (WaterGAP-IPSL-CM5A-LR), (WaterGAP-MIROC-ESM-Chem), and (WaterGAP-NorESM1-M). These models are selected because they have lower RMSE values, higher correlation coefficients, and standard deviation values closer to the model standard deviations. To this end, Figure 4 shows the observed and simulated long-term monthly mean discharge by each of the 25 GCM–GHM combinations. The ensemble means of the simulations across all the GHM forcing combinations show a reasonable fit with the observed streamflow values, with  $R^2$  values of 0.87 and 0.79 in the Ganges and Godavari river basins, respectively. It is observed from Figure 4 that the ensemble mean discharge of the three models selected from the Taylor diagrams shows a better fit with the observed data compared to the 25-model ensemble mean values for both the Ganges and Godavari basins. To know the impact of human activities on seasonality in both of the basins, the long-term monthly mean discharge was calculated and compared under “nosoc” and “pressoc” for the overlapping period of 1971–2000 for each model combination. The average of the long-term mean monthly discharge obtained from the 25 model combinations ( $5\text{GCM} \times 5\text{GHM}$ ) was calculated and plotted as shown in Figure 5. It indicates that the peak flow occurs in August and September in the Godavari and the Ganges, respectively. The percentages of the monthly discharge changes under the “pressoc” condition with respect to the “nosoc” condition for the period 1971–2000 in the two basins are shown in Figure 5. The percentage change is calculated by dividing the increase in the monthly streamflow values (historic nosoc–historic pressoc) by monthly streamflow under the historic nosoc condition and then multiplying it by 100. The percentage change in mean monthly discharges due to human activities during 1971–2000 are observed to be the highest during the pre-monsoon season in both the river basins—these changes generally coincide with the low-flow season, with the river contribution mainly coming from groundwater systems. Furthermore, we find a slightly higher human impact on the Ganges basin than that on the Godavari basin during the pre-monsoon season (Figure 5). The details in the figure might be attributed to the fact that the Ganges is one of the most-populated river basins in the world and water use in that basin is connected with regional social life, culture, agriculture, and demography [24,55]. Conversely, human impact is low during the monsoon and post-monsoon seasons in the both the Ganges and Godavari basins. In the Ganges and Godavari basins, the human impact is highest in May. The results of this analysis in Figure 5 have revealed that the human influences in terms of changes to streamflow in the Godavari river basin is more than that of the Ganges river basin during September, October, and November. This change could be connected with the time delays in the monsoon’s influence on both river basins.

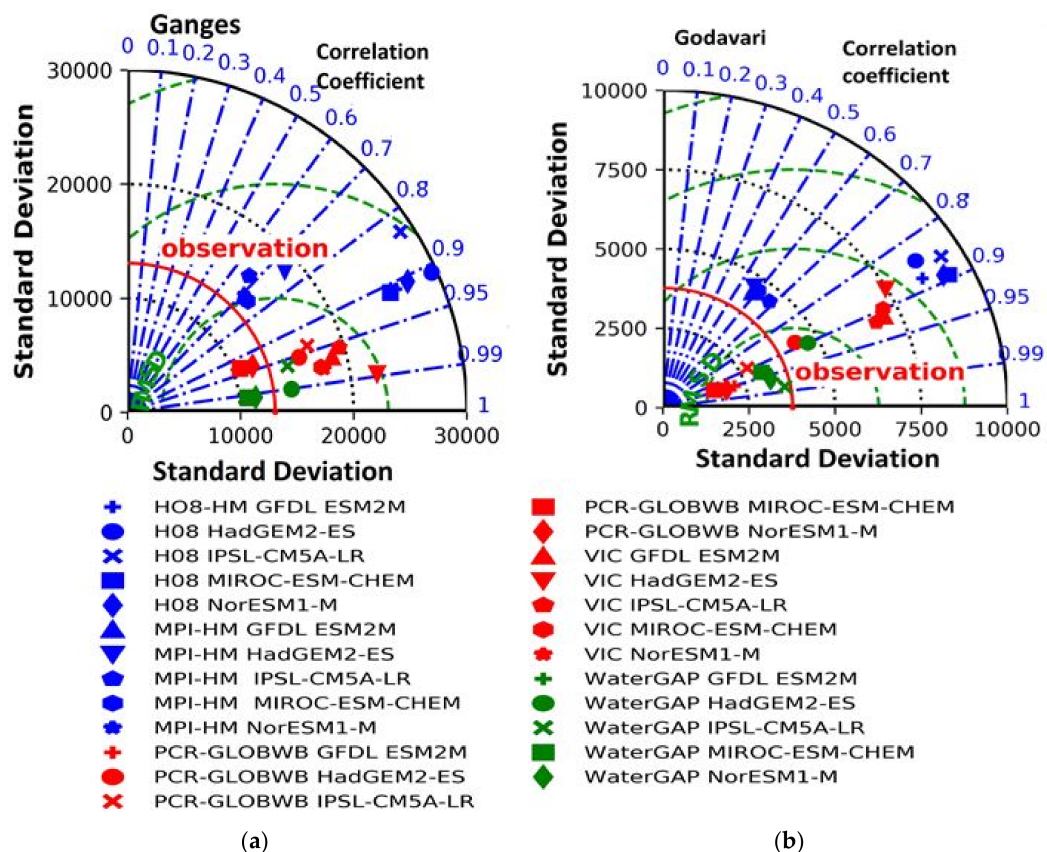


**Figure 3.** Taylor diagrams showing the performance of 25 GCM–GHM combinations for (a) Ganges and (b) Godavari with three different parameters, i.e., RMSE (green dotted lines), standard deviation of model data (black dotted lines), standard deviation of observed data (red line), and correlation coefficient (blue dotted lines).

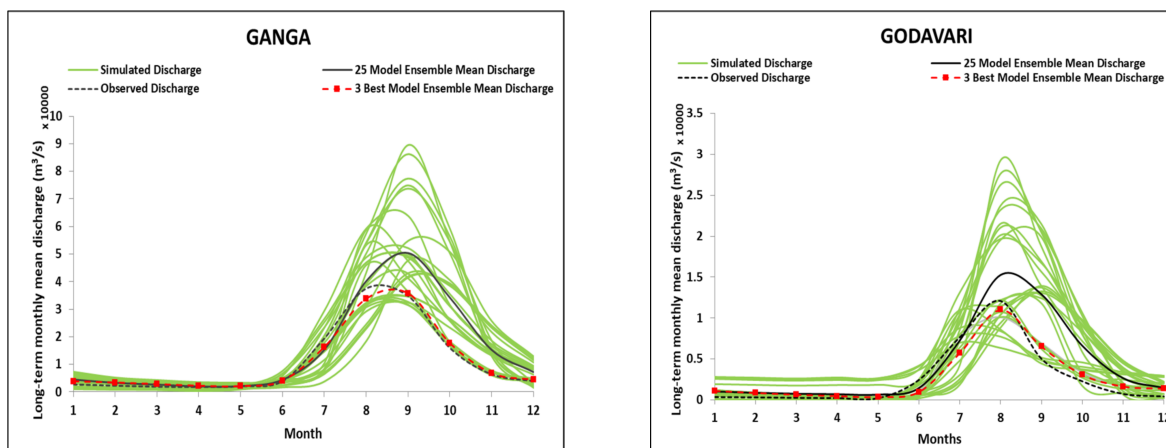


**Figure 4.** Observations and simulations corresponding to long-term mean monthly discharge for the two study basins during the 1971–2000 period. Shown here are the individual model simulations (in green) as well as the multi-model ensemble mean based on the entire (25) and the best three model combinations.

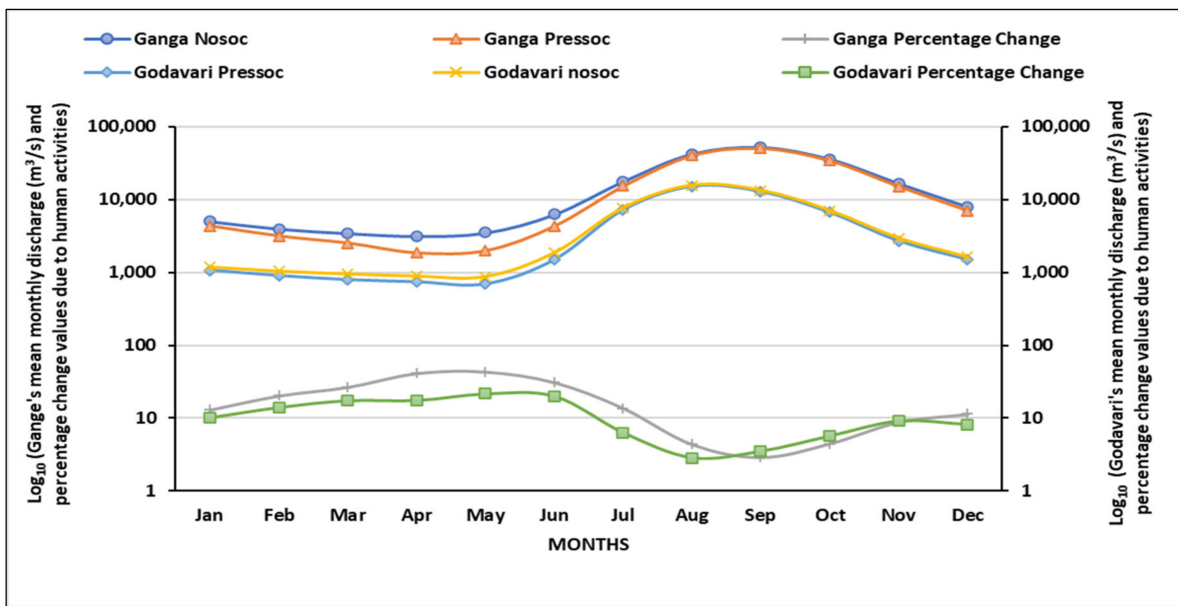


**Figure 5.** Seasonality and percentage change values of streamflow due to human activities in Ganges and Godavari basins (1971–2000 periods).

*3.1. What Attributes Contribute Most to Changes in Seasonal Flows: Current Human Activities or Future Climate Change?*

Figure 6 shows the quantification of the seasonal impact from climate change, comparing the change in the streamflow amount during the near future (2010–39), mid-future (2040–69), and far future (2070–99) for the RCP 2.6 and RCP 8.5 scenarios in relation to the historical period; it is contrasted against the corresponding historical human-induced effect for the two basins. The medians of the absolute relative change in long-term seasonal mean discharge (as discussed in the methodology) obtained from the 25 GCM–GHM combinations are shown with their corresponding 25th percentile and 75th percentile levels (as error bars) in these figures. The median values of relative change in the mean seasonal discharges from the three best GCM–GHM models are detailed in Table 3 to show its bias with the results obtained from the ensemble of 25 GCM–GHM combinations. These figures provide an understanding of (i) how the seasonal net streamflow is sensitive to human activities and climatic changes in different seasonal time slices, and (ii) how close the effect of climate change in the future period is to that of the human activities in the historical period. These differences, according to the main three seasons for both study basins, are discussed below.

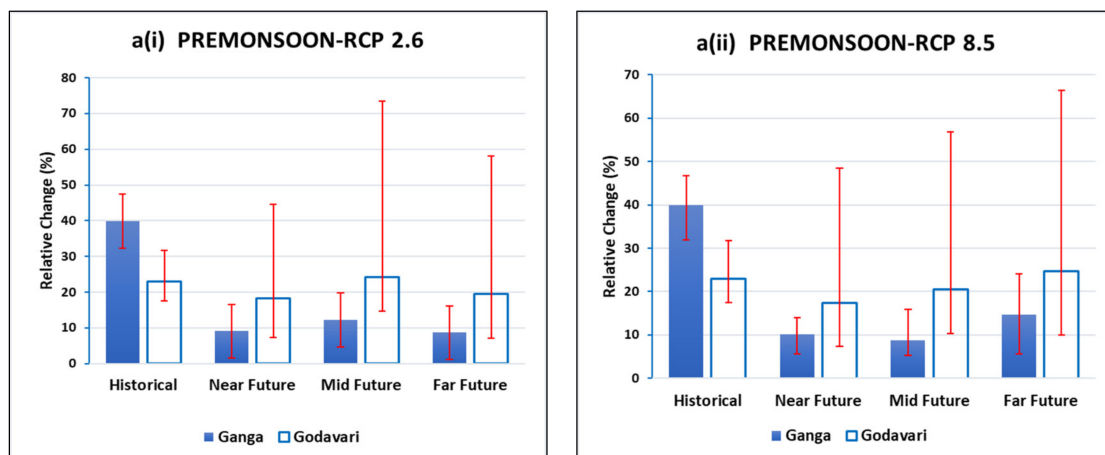


**Figure 6.** Cont.

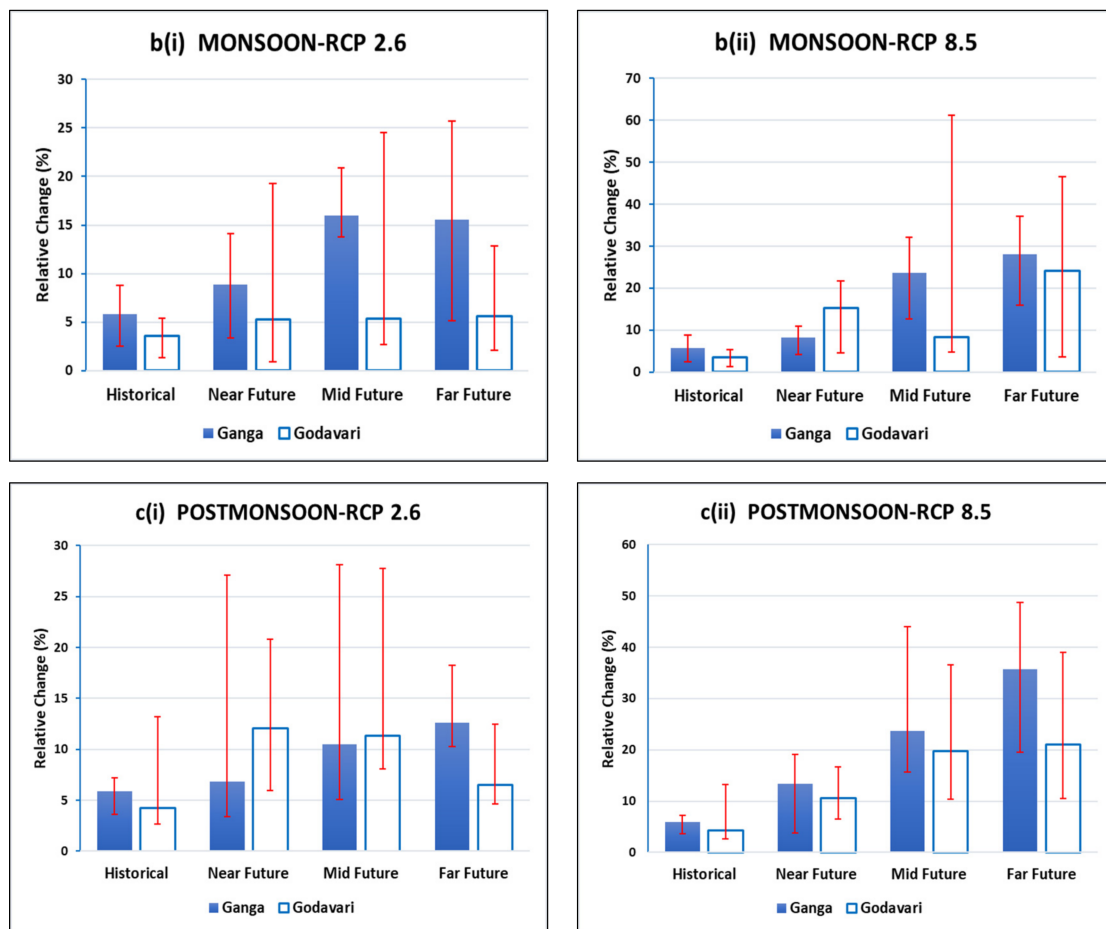


**Figure 6.** Relative change (%) in the long-term mean monthly streamflows due to human impact in the baseline period and climate change impact in the future time slices (under RCP 2.6 and RCP 8.5) during the pre-monsoon, monsoon, and post-monsoon seasons in the Ganges and Godavari basin. Shown here are the median (bar) and the respective 25th and 75th percentile values (red error bars) of the relative changes based on 25 combinations of GCM–GHMs.

### 3.1.1. Pre-Monsoon Season

The first two bars in Figure 6(ai,aii) represent the relative changes in the mean pre-monsoon seasonal flow during the 1971–2000 (historical) period for the Ganges and Godavari river basins. One can note that during the pre-monsoon, human influence in the Ganges has a dominant influence on streamflow change, while climate change has a less significant impact. The effects of human activities on the variation of the pre-monsoon streamflow in the Ganges basin (~40%) is almost 17% higher than that for the Godavari basin (~23%). The impact of climate change on the Ganges basin, under RCP 2.6 during the near future, mid-future, and far future, was on average about 4.4, 3.3, and 4.6 times weaker than the human impact during the baseline period, and it is around 3.9, 4.6, and 2.7 times weaker under RCP 8.5. In the mid-future under RCP 2.6 and far future under RCP 8.5, the climate change impacts on Godavari are slightly stronger (1.05 and 1.08 times, respectively) than the human impacts on streamflow during the baseline period. The median obtained from the three best selected GCM–GHM combinations is on the lower side than that for 25 GCM–GHM combinations. This shows how the models selected based on certain criteria perform differently than the ensemble of all available model combinations.

**Table 3.** Ensemble median (25 member and 3 member) of relative change (%) in seasonal mean flows due to human actions in historical period (refer to Equation (2)) and due to climate change in future time slices (refer to Equation (1)) under RCP 2.6 and RCP 8.5 for the Ganges and Godavari basins. Hist.: Historical period (1971–2000), NF: Near-future period (2010–39), MF: Mid-future period (2040–69), FF: Far-future period (2070–99).

River Basins	Seasons	Ensemble Median	Hist.	RCP 2.6 Scenario			RCP 8.5 Scenario		
				NF	MF	FF	NF	MF	FF
Ganga	Pre-monsoon	25 total members (GCM–GHM)	39.86	9.08	12.24	8.67	10.11	8.72	14.60
	Monsoon		5.79	8.83	15.97	15.52	8.13	23.68	28.12
	Post-monsoon		5.90	6.79	10.50	12.59	13.36	23.65	35.64
	Pre-monsoon	3 best members (GCM–GHM)	33.60	3.61	6.918	5.60	8.93	5.84	6.68
	Monsoon		8.65	14.21	18.35	27.41	10.99	23.68	36.94
	Post-monsoon		22.20	3.35	10.24	12.56	14.06	15.31	26.81
Godavari	Pre-monsoon	25 total members (GCM–GHM)	22.97	18.19	24.20	19.45	17.47	20.60	24.78
	Monsoon		3.54	5.28	5.31	5.56	15.31	8.30	24.09
	Post-monsoon		4.21	12.04	11.31	6.46	10.65	19.76	21.00
	Pre-monsoon	3 best members (GCM–GHM)	25.51	1.09	5.763	3.97	2.66	5.09	6.31
	Monsoon		5.37	4.06	5.11	4.92	5.59	6.56	9.92
	Post-monsoon		18.36	6.02	6.88	3.32	6.70	19.76	16.25

### 3.1.2. Monsoon Season

Figure 6(bi,bii) clearly shows a different trend in both river basins during the monsoon season compared to the pre-monsoon season plots. The climate change impact in the future under both the RCP scenarios dominates the human-induced effect on streamflow during the historical period for both river basins. For the Ganges, the climate change impact follows an increasing trend. Under the RCP 2.6, for the Godavari basin, the future climate change impact is about 1.5 times stronger during all time slices than the historical human impact (~3.5%). Whereas, under the RCP 8.5 scenario, it is more dominating during the far future time slice (6.8 times and ~3.5%). The ensemble median of the relative change values for the streamflow of the Ganges from the three GCM–GHM combinations (selected from the Taylor diagrams) is on the higher side compared to that of the 25-model ensemble median values. However, this trend is not followed during the mid-future period under the RCP 8.5 scenario. For the Godavari basin, the ensemble median values of the three GCM–GHM combinations shows good agreement with the 25-model ensemble median values except for the near-future and far-future period under RCP 8.5.

In general, these results indicate that climate change is one of the main reasons for substantial changes in the future monsoon season streamflow in the two river basins and these changes will be higher than the already experienced streamflow changes due to human activities. The projected streamflow for the Godavari basin shows more uncertainty than the Ganges, which may be due to its geographical location (central India), meaning that it is more affected by monsoon rainfall.

### 3.1.3. Post-Monsoon Season

Figure 6(ci,cii) shows the impacts of human activities on historical streamflow in the Ganges and the Godavari and the climate change impact in the future during the post-monsoon seasons. Climate change has a high impact on streamflow changes in the near future (6.8% (RCP 2.6), 13.36% (RCP 8.5)), mid-future (10.5%, 23.65%), and far future (12.6%, 35.65%), and it is greater than the human impact in the historical period in the Ganges basin (~5.9%). The corresponding changes under the RCP 2.6 and RCP 8.5 scenarios for the Godavari basin were 12.05% and 10.65%, 11.32% and 19.76%, and 6.46% and 21%, for the three timescales, respectively, which is more than the human-induced impact during the historical period (~4.2%). Streamflow change for the Ganges basin under both RCP 2.6 and RCP 8.5 shows an increasing trend. A contrary decreasing trend is observed from the

near future to the far future under the RCP 2.6 scenario for the Godavari basin. For the Ganges basin during the future time slices under RCP 2.6 the ensemble median from the three GCM–GHM combinations shows good agreement with the 25 GCM–GHM model combinations. A large amount of uncertainty in the projected streamflow is observed for the near-future and mid-future time slices under the RCP 2.6 scenario for both the basins.

It is observed that the error bars show a larger variation for the Godavari basin than the Ganges for all the seasons, which signifies that uncertainty over the projected streamflow values is high for the Godavari basin, which may be because the Godavari basin lies in central India and is more vulnerable to changes in monsoon rainfall and scale issues; i.e., the Godavari basin is a smaller basin compared to the Ganges, and the global-scale models may not well represent the basin-scale hydrology.

Overall, to summarize, the historical human impact is high during the pre-monsoon season in both the river basins and is greater than the climate change impact, except for the Godavari basin during the mid-future under RCP 2.6 and during the far future under RCP 8.5. The human impact is more in the Ganges basin compared to the Godavari basin in all three seasons.

High monsoon precipitation during the monsoon season compensates for the reduction in the water levels due to abstraction. Thus, the climate change impact signals dominated over the anthropogenic impact during the monsoon and post-monsoon seasons for both the Ganges and the Godavari under both the RCPs.

### *3.2. How Are the Extreme Flow Indices ( $Q_{90}$ and $Q_{10}$ ) Influenced by Current Human Activities and Future Climate Changes?*

It is interesting to know how low and high flows in these river basins vary under the climate scenarios. Therefore, we analyzed the changes in extreme streamflow conditions to analyze their dependencies on human activities and future climate changes. To analyze this, we computed  $Q_{90}$  (low flow) as the 10th percentile flow, i.e., the flow level that was equaled or exceeded for 90% of the time, and  $Q_{10}$  (high flow) as the 90th percentile flow, i.e., the flow level that is equaled or exceeded for 10% of the time. At the end, we calculated the seasonal values of  $Q_{10}$  and  $Q_{90}$  for the pre-monsoon, monsoon, and post-monsoon during the baseline and three different future timeslots (near future, mid-future, and far future). For each model combination, the absolute relative changes in seasonal  $Q_{10}$  and  $Q_{90}$  due to human actions during the baseline period and due to climate change during the future time slices were calculated using the same expression mentioned in the methodology section. All the 25 values of absolute relative change from each model combination ( $5\text{GHM} \times 5\text{GCM}$ ) are plotted using a box and whisker plot. The ensemble median values from the three best-performing GCM–GHM combinations selected before using the Taylor diagrams for the different seasons and RCPs are given in Tables S1 and S2 (refer to the supporting materials file) and corresponding to the Ganges and the Godavari River basins, respectively. The following section discusses the details of the relative changes in seasonal  $Q_{10}$  (high flows) and  $Q_{90}$  (low flows) due to human activities during the historical period and climate change impacts during the future time slices.

#### *3.2.1. Pre-Monsoon Season*

In the Ganges river basin for the pre-monsoon season, the human-induced effect on extreme flows (both  $Q_{10}$  and  $Q_{90}$ ) during the baseline period is more than the climate change effect during the future time slices under both the RCP 2.6 and RCP 8.5 scenarios (Figure 7(ai,aii)). In the future periods, the climate change impact on high flows ( $Q_{10}$ ) is higher during the mid-future (median value ~16.4%), followed by the near future (~12.1%) and the far future (~6.8%) under RCP 2.6. The climate change impact on low flows ( $Q_{90}$ ) under RCP 2.6 in the Ganges decreases from the near future (13.4%) to the far future (9%). However, under the high emission scenario, the climate change impact on both high flows and low flows reaches the highest by the end of the century. The three-member ensemble median values (Table S1) are lesser than the 25-member ensemble values for high flows

under RCP 2.6 and for low flows under the RCP 8.5 scenario. During the baseline period, the uncertainty when predicting the low flows is higher than that for the high flows. For the high flows, the highest amount of uncertainty when predicting the climate change impact was observed for the mid-future (RCP 2.6) and the far future (RCP 8.5). Similarly, for the future low flow estimates, the near future and mid-future values show more uncertainty under RCP 2.6 and RCP 8.5, respectively.

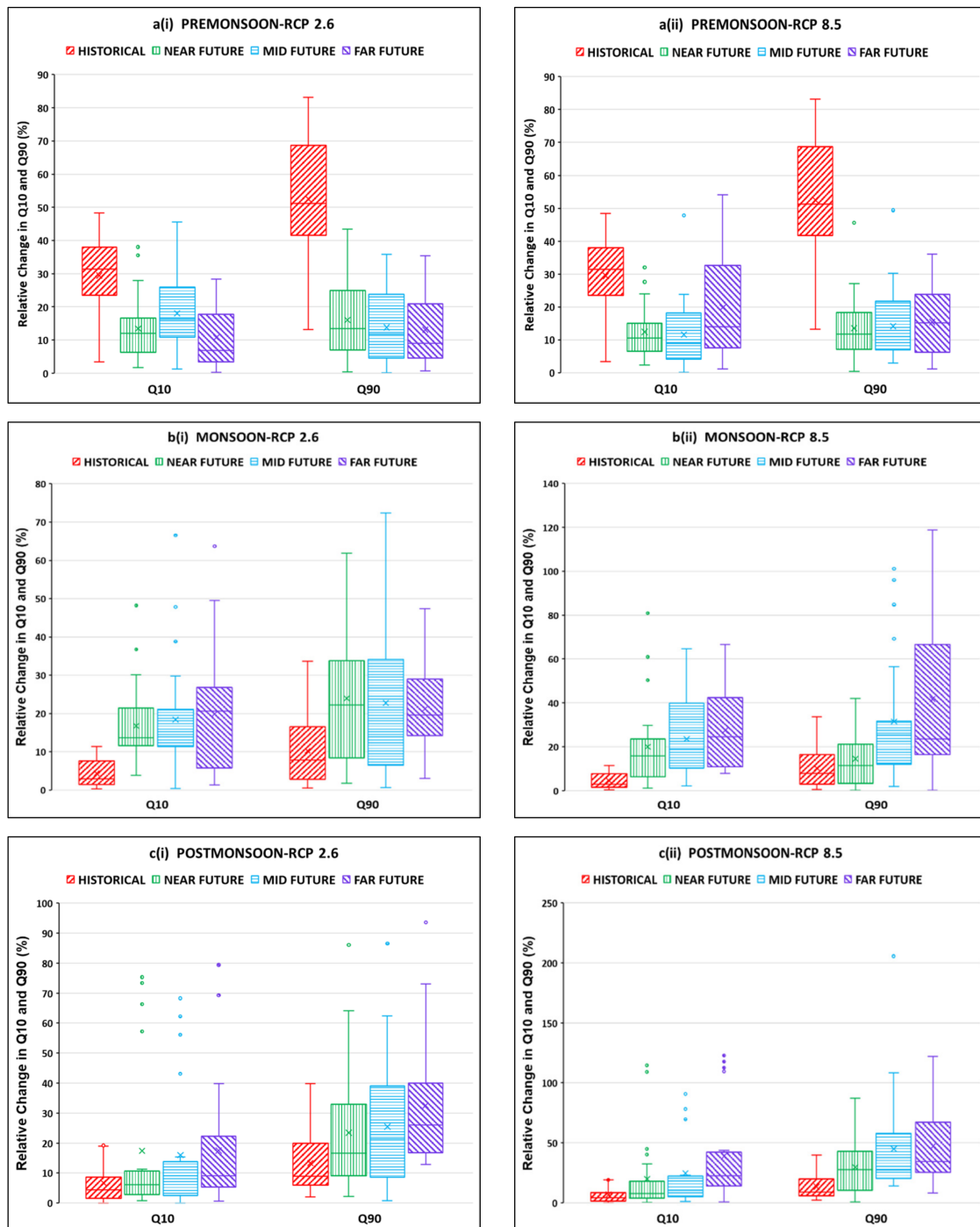


**Figure 7.** Relative change (%) in high flows (Q<sub>10</sub>) and low flows (Q<sub>90</sub>) due to human impact during the baseline period and the climate change impact during the future time slices, i.e., near future, mid-future, and far future (under RCP 2.6 and RCP 8.5) for pre-monsoon, monsoon, and post-monsoon seasons in the Ganges basin. Shown here are the median (bar) and the respective 25th and 75th percentile values (red error bars) of relative changes based on 25 combinations of GCM–GHMs.

For the Godavari river basin (Figure 8(ai,aii)) during the pre-monsoon season, most of the time, the climate change impact during the future is observed to be greater than the human impact (19.9%) during the historical period on high flows, whereas the human impact (36.82%) on low flows was greater than the future climate change impacts under both the RCP 2.6 and RCP 8.5 scenarios. The climate change effect on high flows and low flows shows the highest value during the near future (21.6%) and far future (28.8%), respectively, under RCP 2.6. Under RCP 8.5, the climate change effect on high flows and low flows shows an increasing trend from the near future (18.4% and 15.31%, respectively) to the far future (32.14% and 31.4%, respectively). In the case of the three-member ensemble median (Table S2), the results are lower than the 25-model ensemble median values for both the high and low flows under both the RCP scenarios. Under RCP 2.6 scenario, the highest amount of uncertainty is observed during the near future, and it varied between 1.2% and 652.1% for high flows and 0.52% to 323.52% for low flows. Under RCP 8.5, the peak uncertainty is observed during the far-future period, and it ranged between 2.9% and 1158.1% for high flows, and 2.7% and 281.6% for low flows.

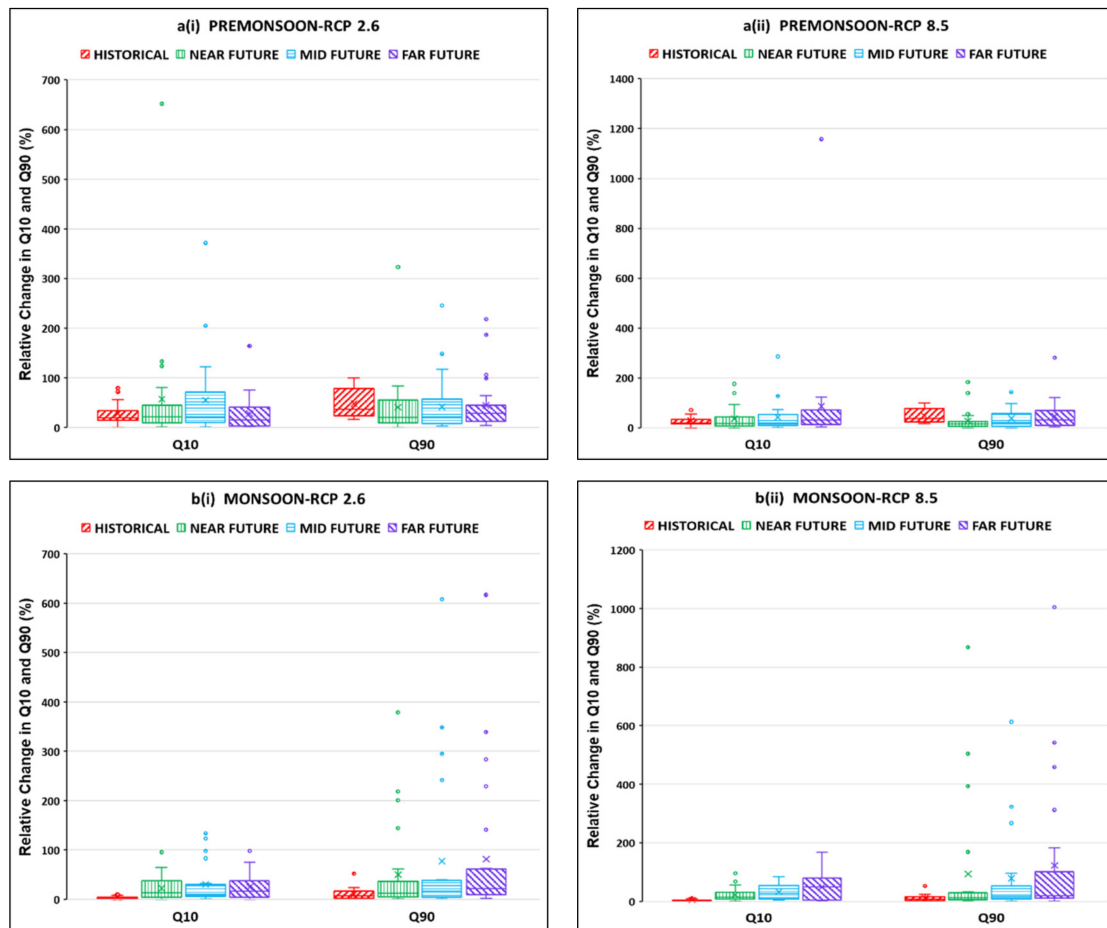
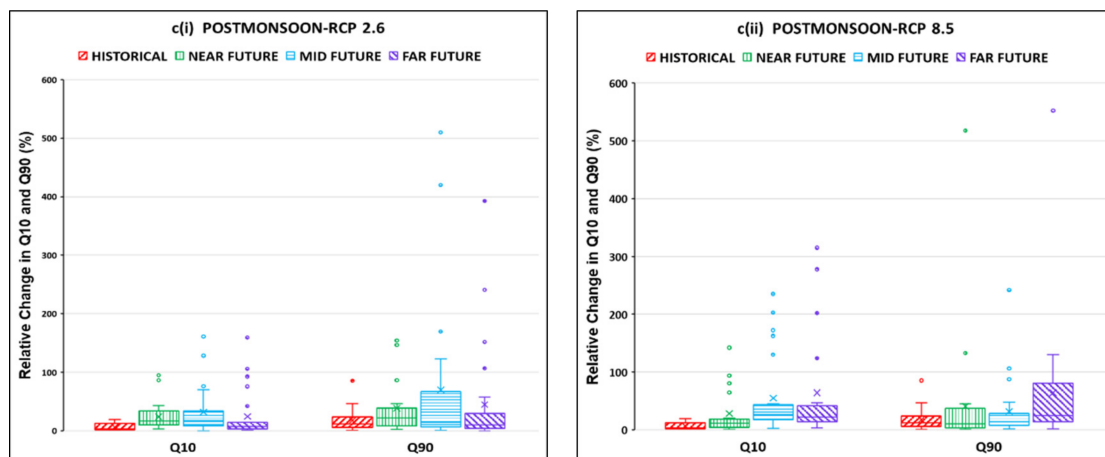


Figure 8. Cont.



**Figure 8.** Relative change (%) in high flows ( $Q_{10}$ ) and low flows ( $Q_{90}$ ) due to human impact during the baseline period and the climate change impact during the future timeslices, i.e., near future, mid-future, and far future (under RCP 2.6 and RCP 8.5) for pre-monsoon, monsoon, and post-monsoon seasons in the Godavari basin. Shown here are the median (bar) and the respective 25th and 75th percentile values (red error bars) of relative changes based on 25 combinations of GCM–GHMs.

### 3.2.2. Monsoon Season

For the Ganges river basin (Figure 7(bi,bii)), the human-induced effect on streamflow during the historical period prevails for low flows (7.8%) compared to high flows (2.9%) in terms of numerical values. The climate change impact on high flows and low flows under both RCP scenarios is greater than the human impact during the historical period. The climate change impact on high flows under both RCP scenarios indicates an increasing trend from the near future to the far future, whereas no such trend is observed in the case of low flows. Slightly more deviation of the three-member ensemble median is observed for low flows during the near future (RCP 2.6) and for high flows during the mid-future and far future under RCP 8.5, and also for the far future under RCP 2.6 (Table S1). Under RCP 2.6, the highest amount of uncertainty is seen during the mid-future for both high flows (ranging from 0.45% to 66.61%) and low flows (ranging from 0.67% to 72.4%). Under RCP 8.5, uncertainty in the estimates of high flows is high for the near future. On the contrary, for low flows, uncertainty is high for the far future (ranging from 0.14% to 118.8%).

For the Godavari basin (Figure 8(bi,bii)) during the monsoon season, the human effect on high flows (3.17%) and low flows (7%) during the baseline period is less significant than the future climate change effect during the future under both RCP 2.6 and RCP 8.5. Under RCP 8.5, the climate change impact on high flows and low flows shows an increasing trend from the near future (15.1% and 11.8%, respectively) to the far future (50.2% and 18.6%, respectively), whereas no such distinctive trend is observed under the RCP 2.6 scenario. The  $Q_{10}$  and  $Q_{90}$  values are high for the far future under both RCPs, which shows that climate change has the highest impact on extreme flows at the end of the century under both of the emission scenarios during the monsoon season. The three-member ensemble median values are lower than those of the 25-member ensemble median values for both high and low flows under both the RCP scenarios for the Godavari basin (Table S2). The uncertainty regarding the historical values of low flows (varying between 0.57% and 52.5%) is more than that for high flows (varying between 0.14% and 15%). Under RCP 2.6 in the Godavari basin, the highest amount of uncertainty is observed for high flows for the mid-future and for low flows for the far future. Uncertainty over the low flow estimates under RCP 8.5 is much higher than for the high flow estimates. The far future values of both high flows and low flows under RCP 8.5 are observed to be the most uncertain for the Godavari basin.

### 3.2.3. Post-Monsoon Season

In the Ganges basin (Figure 7(ci,cii)), the human-induced effect on low flows (9%) is more than that on high flows (4.4%). Conversely, future climate change effects exceeded the human impact, during the historical period, on both high flows and low flows for the RCPs. The projected climate change impact on both high flows and low flows is increasing from the near future to the far future under RCP 2.6 and a similar trend is observed in the case of RCP 8.5. The post-monsoon analysis of the Ganges (Table S1) indicates that the ensemble median of the best selected models shows values which are higher than the 25-model ensemble median values for high flows. A larger amount of uncertainty is observed in the projected climate change impact on high flows for the far-future period, with values ranging from 0.5% to 79.4% under RCP 2.6 and 0.8% to 122.8% under the RCP 8.5 scenario, respectively. Low flow estimates show larger amounts of uncertainty for the mid-future period, which varied from 0.85% to 86.5% and 14.16% to 205.73% under RCP 2.6 and RCP 8.5, respectively.

For the Godavari River basin (Figure 8(ci,cii)), the human impact during the historical period on low flows (11.9%) is more than that on high flows (3.14%). The climate change impact on high flows is highest during the mid-future period, with values of 17.6% and 26.6% under RCP 2.6 and RCP 8.5, respectively. Conversely, the climate change impact on low flows decreases from the near future (22.05%) to the far future (10.18%) under RCP 2.6. For high flows, the three-member ensemble median values are lower than the 25-member ensemble median values for all the future time slices under both of the RCPs (Table S2). The uncertainty over the historical estimates of low flows is greater when compared to the uncertainty over high flows. Under the low emission scenario, the peak of uncertainty in the estimation of high flows (ranging between 0.06% and 161.14%) and low flows (ranging between 1.17% and 509.9%) is observed for the mid-future. Under RCP 8.5, the highest amount of uncertainty occurs for the far future for both high flows (3.37% to 315.1%) and low flows (1.86% to 552.5%).

To summarize the results of the extreme flows analysis, it is observed that in the pre-monsoon season, the human impacts during the baseline period on high flows and low flows overshadowed the climate change impacts (under both RCP 2.6 and RCP 8.5) during the future period for the Ganges basin. For the Godavari basin, most of the time, the future climate change impact on high flows under both RCPs dominated the contemporary human impact. For the monsoon and post-monsoon seasons, the future climate change has a greater impact on high flows and low flows when compared with human impacts during the baseline period for both river basins.

## 4. Discussion

### 4.1. Effect of Human Activities and Climate Change on Seasonal Mean Flows

Earlier studies have focused on the effect of projected climate changes on seasonal streamflow with the help of hydrological model studies, using projected climate data from GCM (global climate model) simulations [53,56,57]. Some researchers have studied the effect of climate change on flood magnitude and timing [58], whereas some studies have focused on analyzing the trend of seasonal flows in the historical period [59,60]. A published study highlighted the effect of climate change on the seasonality of streamflow for the major 11 river basins across the globe, including the Ganges, reporting that climate change will cause an increase in the flows mostly during monsoon season rather than in the pre-monsoon season [53].

In this study, we analyzed the historical human impact on seasonal streamflow and contrasted this to the climate change impact on future seasonal streamflow. This study has focused on highlighting whether a relative change in seasonal streamflow due to human actions in the baseline period is greater or less than the relative change due to climate change effects on future seasonal flows for the Ganges and the Godavari river basins. It is observed that human impacts are more predominant in both the Ganges and Godavari basins during the pre-monsoon season (Figure 6(ai,aii)) compared to the climate change

impact on streamflow during the future period. The streamflow of the Godavari basin during the mid-future and far-future periods under RCP 2.6 and RCP 8.5 shows a slight deviation from this trend. In the Ganges, the human effect (~40%) is more dominating compared to the Godavari (~23%) during the pre-monsoon season, and this may be due to the population difference between the two basins (the population around the Ganges is 329.16 million, and around the Godavari is 60.49 million).

Our study results generally agree with the findings of a previous study [49] that has projected streamflow seasonality, which indicates that streamflow volumes increase in response to monsoonal precipitation in many major global rivers, including the Ganges. Some other previous studies have explored the future tendencies of streamflow during the monsoon season for the Ganges and Godavari basins under the effect of climate change in different scenarios [53,61]. Our study highlights that during the monsoon season, streamflow variation due to climate change increases from the near future to the far future, and this variation is always greater than the change in streamflow due to human actions in the baseline period in both of the river basins. The outputs are in line with the findings of earlier studies [53] on the Ganges which state that the annual streamflow volume increases by +125 mm (+26%) under RCP 8.5 and +77 mm (+16%) under RCP 2.6. The huge uncertainty in the simulations in our study is in agreement with the observations made by other researchers [62], indicating that water resource responses to climate change are hugely dependent on data and information sources, climate models, and hydrological models. However, here, we did not focus on the quantification of the corresponding future impact of human activity on streamflow and the influence of its dampening or magnification effects on streamflow, as the model runs without considering changes in future human activities (socio-economic conditions) because these are not considered in this study for the selected ISIMIP model runs. Some studies from the Brazilian Amazon that assess future human activities in terms of land-use change partially counteract the climate-driven diminishing trend in river flows [63]. Thus, we have considered an evaluation of how future anthropogenic disturbances in water use and land-cover dynamics would influence the river flows of the Ganges and the Godavari to be the future scope of this work to see how the inter-annual and intra-annual flow variability would change under such settings and also to see the combined effect of human activities and climate change.

An earlier analysis performed by researchers [64] has shown that surface runoff is projected to increase in the majority of the sub-continental river basins in post-monsoon seasons. In the current study, in the post-monsoon season in both river basins, the variation in future streamflow due to climate change is greater than the variation due to human actions in the historical period. During the post-monsoon season, in the Ganges basin, streamflow variation under RCP 2.6 and RCP 8.5 shows an increasing trend, which shows how climate change has a more dominant effect in the far future. In the case of the Godavari basin under RCP 2.6 scenarios, the climate change impact on streamflow decreases from the near future to the far future, whereas, on the contrary, it shows an increasing trend from the near future to the far future when observed under the RCP 8.5 emission scenario. The values corresponding to the Ganges during the post-monsoon were 12.2%, 22.5%, and 36.9% for the RCP 8.5 scenario during the three time slices, respectively. The corresponding post-monsoon RCP 8.5 projected runoff values were 17.6%, 25%, and 72% in the Godavari during 2010–2039, 2040–2069, and 2070–2099, respectively. Our study results indicate that the larger amount of uncertainty regarding the precipitation projections from the GCMs are translated to the GHMs seasonal simulations as reported in the prior study conducted by our group of investigators [65]. Uncertainty in the future streamflow prediction is observed to be more for the Godavari compared to the Ganges, which may be due to the fact that the Godavari is in central India and, therefore, is more exposed to the early influence of monsoonal precipitation during the early summer months. There is also a lack of glacier reserves in the basin.

#### 4.2. Effect of Human Activities and Climate Change on Seasonal Extremes (High Flows and Low Flows)

In the literature, most of the studies on global rivers focused only on the examination of the effect of climate change alone on streamflow [66–69]. Some of the exceptions are those focusing on assessing (i) the effect of human activities and climate change on streamflow [3,70], (ii) how human water management is intensifying the hydrological drought [71], (iii) how streamflow is affected by land-use change along with climate change [72], and (iv) how multiple river flow characteristics are influenced by choices of multiple GCM and GHM scenarios [73]. In our study, an effort has been made to understand the impact of climate change on high flows and low flows and then to contrast this with the impact of human action on these extreme flows during the contemporary period. A similar attempt has been made by scholars earlier [74] to assess how the combined impact of human water use and climate change results in water stress and surface water availability in Iran. Some researchers have studied [61] how high flows become affected by climate change during the future period as compared to the historical period for the Godavari basin and reported the observation that high flows increase in the future, and this upsurge is greater under the RCP 8.5 than the RCP 2.6 scenario. The same trend is observed in our study, with the effect of climate change on extreme flows the highest during the far future for the Godavari basin under the RCP 8.5 scenario, showing relative change values of 32.15% (high flows) and 31.36% (low flows) in the pre-monsoon season, 50.19% and 18.59%, respectively, in the monsoon season, and 24.31% for low flows in the post-monsoon season. This trend is not followed by the post-monsoon season (26.58%) for high flows, as the climate change impact during the mid-future is dominating. However, our study focuses on analyzing the impact of human actions and climate change on extreme flows in terms of absolute relative change and does not aim to quantify the increasing or decreasing trend of extreme flow values.

An earlier study has highlighted that uncertainty regarding changes in long-term average river discharges in terms of Q10, Q50, and Q90 in the monsoon-dominated basins are dependent on GCMs–HMs–RCPs combinations and the nature of the river [75]. Researchers have analyzed the impact of climate change on the future flows of 12 major river basins worldwide and, in the context of the Ganges, reported an increasing trend in high flows under RCP 8.5 by the end of this century [49]. A similar trend is observed in our analysis, showing the larger impact of climate change on high flows as well as on low flows for the far future in the Ganges under the RCP 8.5 emission scenario with values of 13.9% and 15.1%, respectively, during the pre-monsoon season and 22.85% and 34.4%, respectively, during the post-monsoon season. During the monsoon season, the same trend is followed by high flows with a value 24.4%, but low flows (25.35%) show slight deviation and are more affected in the mid-future period. Greater disturbances with low flows are observed during the near future for both the pre-monsoon (13.4%) and the monsoon (22.3%) seasons, whereas for the post-monsoon season (26%), it is highest during the far future under RCP 2.6 for the Ganges basin.

A comparative analysis of the extreme flows of both the river basins shows that during the pre-monsoon season, the anthropogenic impact on high flow and low flow is more than the future climate change impact for the Ganges, whereas this is applicable for low flows only in case of the Godavari basin. In the monsoon and post-monsoon seasons, the climate change impact during the future time slices dominates in comparison to the human impact during the current period for both river basins.

#### A Word of Caution

Though ISIMIP is a well-studied framework and data source, many studies have highlighted its total uncertainty for assessing future climate impacts [76,77] and uncertainties over human impact considerations [78]. The GCMs and GHMs considered in this study also have their own uncertainties connected with the model structure and scenario designs. Apart from that, this kind of study, focusing on small subsets of the CMIP5, can be expected to underestimate both the total uncertainty of the future climate impact [78]. It must also be

stressed that uncertainty must be translated and attributed to different the GHMs used for these two river basins. In this study, we have performed the cross-checking of effectiveness of the GHM simulations with a limited amount of data due to the classified nature of the Ganges River basin and other data-related constraints. Even though we are relying on the previously simulated ISIMIP datasets, which are well-established in the impact community, the evaluation outputs will be more meaningful if we make a validation with longer flow datasets from different gauging locations in the river basins to see how well the ISIMIP GCMs and GHMs perform during the baseline period. The inclusions of human impact parameterizations in different ISIMIP GHMs are rather simple in nature and are different from one another. These differences in the parameterization of human impacts, which are associated with between-model uncertainties, will have an influence on the findings of such subset studies that focus on five CMIP5 models, as shown here. However, detailed investigation of the connection between the model uncertainty resulting from the inclusion of human impact parameterizations and subsequent simulated river flows are well studied by some researchers [78]. Therefore, we urge the data users to consider how such uncertainty differences exist between the two experiments (i.e., 'pressoc' and 'nosoc') when they are used for hydrological impact assessments, policy implications, and related management decisions. We must also consider the uniformity of human impact parameterizations among the GHMs and their detailed representations in the GHM modules. Only then will the analyses similar to this study become more meaningful for a better understanding of future water flow in Indian river basins with regional variations and contrasting human influences. More detailed and elaborate human impact scenarios need to be taken into consideration for better realistic estimates, in which the human influences also change in the future in conjunction with climate change, something which is lacking in this study. Thus, the findings and outcomes from this study may be considered to be one of the possible water flow scenarios with a rather low probability of human impact, as current ISIMIP or impact model runs do not provide those runs with elaborate considerations of all possible human impacts. The ISIMIP GHMs are calibrated with limited regional flow datasets, which itself highlights the need for the comprehensive calibration of GHMs for better and more reliable simulations of regional river basins. However, we expect that more robust and confidential future projections of river regime changes under a changing climate, and human impact tendencies with more regional focus, will arrive in the future, with widespread use of ISIMIP3a and its successive data sources. Another point to note is that in this study, the specific application of GHMs is not calibrated at the basin scale. Though it is a well-accepted fact that the global- and continental-scale models are mostly applied using a multi-model ensemble with minimal basin-scale calibration, some studies have highlighted that the basin-scale calibration of GHMs could improve their credibility of streamflow projections [79]. Further incorporation of post-processing techniques, such as Bayesian model averages, can help to improve the accuracy of model simulations in studies similar to this case study from the Ganges and Godavari basins.

## 5. Conclusions

The goal of this study was to assess and compare the impact of climate change during three different future timeslots with human-induced impacts during the historical period on long-term seasonal mean flows and seasonal extreme flows (low flow and high flow) in two contrasting Indian river basins. Based on the results of our study, the main conclusions drawn can be summarized as:

- The best performing GCM–GHM model combinations based on observations from the Taylor diagrams for the Ganges are (WaterGAP-NorESM1-M), (WaterGAP-MIROC-ESM-Chem), and (WaterGAP-HADGEM2-ES), and for the Godavari, (WaterGAP-IPSL-CM5A-LR), (WaterGAP-MIROC-ESM-Chem), and (WaterGAP-NorESM1-M). The ensemble mean monthly streamflow from these combinations shows good agreement with the observed data, with correlation coefficients ranging between 0.93 and 0.99.

- During the pre-monsoon season, the historical human impacts on long-term seasonal discharge in the Ganges and Godavari River basins are around 40% and 23%, respectively, which is mostly greater than the climate change impact during the future. Likewise, it is also more than the contemporary human impact during the monsoon and post-monsoon seasons for both the basins, though it could be due to less irrigation requirements during the monsoon and post-monsoon periods in the Himalayan perennial river (the Ganges) and the sub-continental non-perennial river (the Godavari). On the other hand, during the monsoon and post-monsoon seasons, the climate change impact during the future period is higher compared to the human impact during the historical period.
- For both the Ganges and Godavari basins, under the RCP 8.5 scenario, the climate change impact during the far-future period is strictly more than during the other future time slices under both of the RCPs. For the Ganges, it is highest during the far-future period for post-monsoon season (~35.6%) and for the Godavari, it is at its maximum during the far-future period for the pre-monsoon season (~24.8%).
- The human impact during the historical period on both high flows and low flows is greater during the pre-monsoon season compared to the monsoon and post-monsoon season in both the river basins.
- During the pre-monsoon season, both high flows and low flows become more affected by human action in the baseline period compared to the climate change impact during the future periods for both the basins. The exception is for the Godavari, where, for most of the time, the climate change impact on high flows under both the RCP scenarios overshadowed the contemporary human impact.
- For the monsoon season, high flows show the most disturbance during far future, with values increased to 20.7% and 24.4% in the Ganges basin, and 16.3% and 50.2% in the Godavari River basin under both the RCP 2.6 and RCP 8.5 scenarios, respectively.
- Under the RCP 8.5 scenario in the post-monsoon season, for the Ganges basin, the climate change impact during the far future is dominant on both high flows (22.8%) and low flows (34.4%), whereas in the Godavari basin, the highest impact of climate change on high flows is observed during the mid-future (26.6%) and on low flows, it is during the far future (24.3%).
- Uncertainty in the streamflow estimates is observed to be greater for the Godavari basin for both the long-term seasonal mean discharge values and extreme flow values compared to the Ganges.

**Supplementary Materials:** The following supporting information can be downloaded at: <https://www.mdpi.com/article/10.3390/w14020194/s1>, Table S1: Ensemble median (25 member and 3 member) of relative change (%) in high flow (Q10) and low flow (Q90) during historical period due to human action (refer equation 2) and during future time slices due to climate change (refer equation 1) under RCP2.6 and RCP8.5. for the Ganges basin; Table S2: Ensemble median (25 member and 3 member) of relative change (%) in high flow (Q10) and low flow (Q90) during historical period due to human action (refer equation 2) and during future time slices due to climate change (refer equation 1) under RCP2.6 and RCP8.5 for the Godavari basin.

**Author Contributions:** Conceptualization, R.R. and R.K.; methodology, R.R. and R.K.; formal analysis, A.S. and A.P.; data curation, A.S. and A.P.; writing—original draft preparation, R.R. and A.S.; writing—review and editing, R.R., R.K. and A.P.; supervision, R.R. and R.K.; project administration, R.R. and R.K.; funding acquisition, A.S., R.R. and R.K. All authors have read and agreed to the published version of the manuscript.

**Funding:** This research was funded by the German Academic Exchange Service (DAAD) in 2019 with a grant number #91755431.

**Data Availability Statement:** Publicly available datasets were analyzed in this study. This data can be found here: <https://portal.grdc.bafg.de/applications/public.html?publicuser=PublicUser#dataDownload/Home> accessed on 15 october 2019; <https://indiawrri.gov.in/wrri/> accessed on

6 November 2019; <https://www.isimip.org/outputdata/isimip-data-on-the-esgf-server/> accessed on 20 May 2019.

**Acknowledgments:** Authors are thankful to IIT Kharagpur, TU Dresden, and UFZ Leipzig for administrative support and to Er. Avijit Majhi for technical support. For their roles in producing, coordinating, and making available the ISIMIP input data and impact model output, we acknowledge the modelling groups, the ISIMIP sector coordinators, and the ISIMIP cross-sectoral science team for the Water Global sector (GHMs are listed in Table 2 of this paper—the model simulations are based on the ISIMIP fast track). We would like to thank Aiendril Dey, IIT Kharagpur for helping with Taylor diagram mapping and analysis.

**Conflicts of Interest:** The authors declare no conflict of interest.

## References

- Ahn, K.H.; Merwade, V. Quantifying the relative impact of climate and human activities on streamflow. *J. Hydrol.* **2014**, *515*, 257–266. [[CrossRef](#)]
- Haslinger, K.; Koffler, D.; Schöner, W.; Laaha, G. Exploring the link between meteorological drought and streamflow: Effects of climate-catchment interaction. *Water Resour. Res.* **2014**, *50*, 2468–2487. [[CrossRef](#)]
- Zhang, D.; Zhang, Q.; Qiu, J.; Bai, P.; Liang, K.; Li, X. Intensification of hydrological drought due to human activity in the middle reaches of the Yangtze River, China. *Sci. Total Environ.* **2018**, *637–638*, 1432–1442. [[CrossRef](#)]
- Huang, J.C.; Lin, C.C.; Chan, S.C.; Lee, T.Y.; Hsu, S.C.; Lee, C.T.; Lin, J.C. Stream discharge characteristics through urbanization gradient in Danshui River, Taiwan: Perspectives from observation and simulation. *Environ. Monit. Assess.* **2012**, *184*, 5689–5703. [[CrossRef](#)]
- Liu, X.; Liu, W.; Yang, H.; Tang, Q.; Flörke, M.; Masaki, Y.; Müller Schmied, H.; Ostberg, S.; Pokhrel, Y.; Satoh, Y.; et al. Multimodel assessments of human and climate impacts on mean annual streamflow in China. *Hydrol. Earth Syst. Sci.* **2019**, *23*, 1245–1261. [[CrossRef](#)]
- Warszawski, L.; Frieler, K.; Huber, V.; Piontek, F.; Serdeczny, O.; Schewe, J. The inter-sectoral impact model intercomparison project (ISI-MIP): Project framework. *Proc. Natl. Acad. Sci. USA* **2014**, *111*, 3228–3232. [[CrossRef](#)]
- Rosenzweig, C.; Arnell, N.W.; Ebi, K.L.; Lotze-Campen, H.; Raes, F.; Rapley, C.; Smith, M.S.; Cramer, W.; Frieler, K.; Reyer, C.P.O.; et al. Assessing inter-sectoral climate change risks: The role of ISIMIP. *Environ. Res. Lett.* **2017**, *12*, 010301. [[CrossRef](#)]
- Wanders, N.; Wada, Y. Human and climate impacts on the 21st century hydrological drought. *J. Hydrol.* **2015**, *526*, 208–220. [[CrossRef](#)]
- Arheimer, B.; Donnelly, C.; Lindström, G. Regulation of snow-fed rivers affects flow regimes more than climate change. *Nat. Commun.* **2017**, *8*, 62. [[CrossRef](#)]
- Veldkamp, T.I.E.; Zhao, F.; Ward, P.J.; De Moel, H.; Aerts, J.C.J.H.; Schmied, H.M.; Portmann, F.T.; Masaki, Y.; Pokhrel, Y.; Liu, X.; et al. Human impact parameterizations in global hydrological models improve estimates of monthly discharges and hydrological extremes: A multi-model validation study. *Environ. Res. Lett.* **2018**, *13*, 055008. [[CrossRef](#)]
- Prudhomme, C.; Giuntoli, I.; Robinson, E.L.; Clark, D.B.; Arnell, N.W.; Dankers, R.; Fekete, B.M.; Franssen, W.; Gerten, D.; Gosling, S.N.; et al. Hydrological droughts in the 21st century, hotspots and uncertainties from a global multimodel ensemble experiment. *Proc. Natl. Acad. Sci. USA* **2014**, *111*, 3262–3267. [[CrossRef](#)]
- Wada, Y.; Van Beek, L.P.H.; Bierkens, M.F.P. Modelling global water stress of the recent past: On the relative importance of trends in water demand and climate variability. *Hydrol. Earth Syst. Sci.* **2011**, *15*, 3785–3808. [[CrossRef](#)]
- Wada, Y.; Wisser, D.; Bierkens, M.F.P. Global modeling of withdrawal, allocation and consumptive use of surface water and groundwater resources. *Earth Syst. Dyn.* **2014**, *5*, 15–40. [[CrossRef](#)]
- Wada, Y.; Van Beek, L.P.H.; Van Kempen, C.M.; Reckman, J.W.T.M.; Vasak, S.; Bierkens, M.F.P. Global depletion of groundwater resources. *Geophys. Res. Lett.* **2010**, *37*, L20402. [[CrossRef](#)]
- Nijssen, B.; O'Donnell, G.M.; Lettenmaier, D.P.; Lohmann, D.; Wood, E.F. Predicting the discharge of global rivers. *J. Clim.* **2001**, *14*, 3307–3323. [[CrossRef](#)]
- Liang, X.; Lettenmaier, D.P.; Wood, E.F.; Burges, S.J. A simple hydrologically based model of land surface water and energy fluxes for general circulation models. *J. Geophys. Res.* **1994**, *99*, 14415–14428. [[CrossRef](#)]
- Hanasaki, N.; Inuzuka, T.; Kanae, S.; Oki, T. An estimation of global virtual water flow and sources of water withdrawal for major crops and livestock products using a global hydrological model. *J. Hydrol.* **2010**, *384*, 232–244. [[CrossRef](#)]
- Hanasaki, N.; Yoshikawa, S.; Pokhrel, Y.; Kanae, S. A global hydrological simulation to specify the sources of water used by humans. *Hydrol. Earth Syst. Sci.* **2018**, *22*, 789–817. [[CrossRef](#)]
- Rao, R.G. Climate change mitigation through reforestation in Godavari mangroves in India. *Int. J. Clim. Chang. Strateg. Manag.* **2009**, *1*, 340–355. [[CrossRef](#)]
- Jhajharia, D.; Dinpashoh, Y.; Kahya, E.; Choudhary, R.R.; Singh, V.P. Trends in temperature over Godavari River basin in Southern Peninsular India. *Int. J. Climatol.* **2014**, *34*, 1369–1384. [[CrossRef](#)]

21. Döll, P.; Hoffmann-Dobrev, H.; Portmann, F.T.; Siebert, S.; Eicker, A.; Rodell, M.; Strassberg, G.; Scanlon, B.R. Impact of water withdrawals from groundwater and surface water on continental water storage variations. *J. Geodyn.* **2012**, *59–60*, 143–156. [[CrossRef](#)]
22. Ramesh, R.; Lakshmi, A.; Sappal, S.M.; Bonthu, S.R.; Suganya, M.D.; Ganguly, D.; Robin, R.S.; Purvaja, R. Integrated Management of the Ganges Delta, India. In *Coasts and Estuaries*; Elsevier: Amsterdam, The Netherlands, 2019; pp. 187–211. [[CrossRef](#)]
23. Roy, P.S.; Meiyappan, P.; Joshi, P.K.; Kale, M.P.; Srivastav, V.K.; Srivasatava, S.K.; Krishnamurthy, Y.V.N. Decadal Land Use and Land Cover Classifications across India, 1985, 1995, 2005. Available online: [Daac.ornl.gov](http://Daac.ornl.gov) (accessed on 10 December 2019).
24. CWC. NRSC Ganga Basin Report. 2011. Available online: [https://www.nrsc.gov.in/sites/default/files/pdf/Announcements/Glacial\\_Lake\\_Atlas\\_Ganga\\_Basin\\_NRSC.pdf](https://www.nrsc.gov.in/sites/default/files/pdf/Announcements/Glacial_Lake_Atlas_Ganga_Basin_NRSC.pdf) (accessed on 13 June 2019).
25. GRMB. Available online: <http://grmb.gov.in/grmb/basin> (accessed on 1 September 2021).
26. CWC; NRSC. *Godavari Basin Report Version 2.0*; Ministry of Water Resources, Government of India: New Delhi, India, 2014.
27. KPMG India Economic Survey 2015–2016—Key Highlights. 2016. Available online: <https://assets.kpmg/content/dam/kpmg/pdf/2016/04/KPMG-Flash-News-India-Economic-Survey-2015-16%E2%80%93Key-Highlights-3.pdf> (accessed on 14 June 2019).
28. World Food and Agriculture. *Statistical Yearbook 2020*; FAO: Rome, Italy, 2020.
29. Ambika, A.K.; Wardlow, B.; Mishra, V. Remotely sensed high resolution irrigated area mapping in India for 2000 to 2015. *Sci. Data* **2016**, *3*, 160118. [[CrossRef](#)]
30. Hanasaki, N.; Kanae, S.; Oki, T.; Masuda, K.; Motoya, K.; Shirakawa, N.; Shen, Y.; Tanaka, K. An integrated model for the assessment of global water resources—Part 1: Model description and input meteorological forcing. *Hydrol. Earth Syst. Sci.* **2008**, *12*, 1007–1025. [[CrossRef](#)]
31. Hanasaki, N.; Kanae, S.; Oki, T.; Masuda, K.; Motoya, K.; Shirakawa, N.; Shen, Y.; Tanaka, K. An integrated model for the assessment of global water resources—Part 2: Applications and assessments. *Hydrol. Earth Syst. Sci.* **2008**, *12*, 1027–1037. [[CrossRef](#)]
32. Hanasaki, N.; Fujimori, S.; Yamamoto, T.; Yoshikawa, S.; Masaki, Y.; Hijioka, Y.; Kainuma, M.; Kanamori, Y.; Masui, T.; Takahashi, K.; et al. A global water scarcity assessment under Shared Socio-economic Pathways—Part 2: Water availability and scarcity. *Hydrol. Earth Syst. Sci.* **2013**, *17*, 2393–2413. [[CrossRef](#)]
33. Hagemann, S.; Dümenil Gates, L. Validation of the hydrological cycle ECMWF and NCEP reanalyses using the MPI hydrological discharge model. *J. Geophys. Res. Atmos.* **2001**, *106*, 1503–1510. [[CrossRef](#)]
34. Van Beek, L.P.H.; Wada, Y.; Bierkens, M.F.P. Global monthly water stress: 1. Water balance and water availability. *Water Resour. Res.* **2011**, *47*, W07518. [[CrossRef](#)]
35. Wada, Y.; Van Beek, L.P.H.; Wanders, N.; Bierkens, M.F.P. Human water consumption intensifies hydrological drought worldwide. *Environ. Res. Lett.* **2013**, *8*, 034036. [[CrossRef](#)]
36. Nijssen, B.; Schnur, R.; Lettenmaier, D.P. Global retrospective estimation of soil moisture using the variable infiltration capacity land surface model, 1980–1993. *J. Clim.* **2001**, *14*, 1790–1808. [[CrossRef](#)]
37. Irannejad, P.; Henderson-Sellers, A. Evaluation of AMIP II global climate model simulations of the land surface water budget and its components over the GEWEX-CEOP regions. *J. Hydrometeorol.* **2007**, *8*, 304–326. [[CrossRef](#)]
38. Alcamo, J.; Henrichs, T. Critical regions: A model-based estimation of world water resources sensitive to global changes. *Aquat. Sci.* **2002**, *64*, 352–362. [[CrossRef](#)]
39. Schmied, H.M.; Eisner, S.; Franz, D.; Wattenbach, M.; Portmann, F.T.; Flörke, M.; Döll, P. Sensitivity of simulated global-scale freshwater fluxes and storages to input data, hydrological model structure, human water use and calibration. *Hydrol. Earth Syst. Sci.* **2014**, *18*, 3511–3538. [[CrossRef](#)]
40. Döll, P.; Siebert, S. Global modeling of irrigation water requirements. *Water Resour. Res.* **2002**, *38*, 8-1–8-10. [[CrossRef](#)]
41. Döll, P.; Kaspar, F.; Lehner, B. A global hydrological model for deriving water availability indicators: Model tuning and validation. *J. Hydrol.* **2003**, *270*, 105–134. [[CrossRef](#)]
42. Werth, S.; Güntner, A.; Petrovic, S.; Schmidt, R. Integration of GRACE mass variations into a global hydrological model. *Earth Planet. Sci. Lett.* **2009**, *277*, 166–173. [[CrossRef](#)]
43. Döll, P.; Fiedler, K.; Zhang, J. Global-scale analysis of river flow alterations due to water withdrawals and reservoirs. *Hydrol. Earth Syst. Sci.* **2009**, *13*, 2413–2432. [[CrossRef](#)]
44. Werth, S.; Güntner, A. Calibration analysis for water storage variability of the global hydrological model WGHM. *Hydrol. Earth Syst. Sci.* **2010**, *14*, 59–78. [[CrossRef](#)]
45. Fritsche, M.; Döll, P.; Dietrich, R. Global-scale validation of model-based load deformation of the Earth’s crust from continental watermass and atmospheric pressure variations using GPS. *J. Geodyn.* **2012**, *59–60*, 133–142. [[CrossRef](#)]
46. Jin, S.; Feng, G. Large-scale variations of global groundwater from satellite gravimetry and hydrological models, 2002–2012. *Glob. Planet. Change* **2013**, *106*, 20–30. [[CrossRef](#)]
47. Döll, P.; Fritsche, M.; Eicker, A.; Müller Schmied, H. Seasonal Water Storage Variations as Impacted by Water Abstractions: Comparing the Output of a Global Hydrological Model with GRACE and GPS Observations. *Surv. Geophys.* **2014**, *35*, 1311–1331. [[CrossRef](#)]
48. Hempel, S.; Frieler, K.; Warszawski, L.; Schewe, J.; Piontek, F. A trend-preserving bias correction—the ISI-MIP approach. *Earth Syst. Dyn.* **2013**, *4*, 219–236. [[CrossRef](#)]

49. Krysanova, V.; Vetter, T.; Eisner, S.; Huang, S.; Pechlivanidis, I.; Strauch, M.; Gelfan, A.; Kumar, R.; Aich, V.; Arheimer, B.; et al. Intercomparison of regional-scale hydrological models and climate change impacts projected for 12 large river basins worldwide—A synthesis. *Environ. Res. Lett.* **2017**, *12*, 105002. [[CrossRef](#)]
50. Almazroui, M.; Saeed, S.; Saeed, F.; Islam, M.N.; Ismail, M. Projections of Precipitation and Temperature over the South Asian Countries in CMIP6. *Earth Syst. Environ.* **2020**, *4*, 297–320. [[CrossRef](#)]
51. ISIMIP2a. Available online: <https://www.isimip.org/protocol/2a/> (accessed on 1 September 2021).
52. Telteu, C.E.; Müller Schmied, H.; Thiery, W.; Leng, G.; Burek, P.; Liu, X.; Boulange, J.E.S.; Andersen, L.S.; Grillakis, M.; Gosling, S.N.; et al. Understanding each other's models An introduction and a standard representation of 16 global water models to support intercomparison, improvement, and communication. *Geosci. Model Dev.* **2021**, *14*, 3843–3878. [[CrossRef](#)]
53. Eisner, S.; Flörke, M.; Chamorro, A.; Daggupati, P.; Donnelly, C.; Huang, J.; Hundecha, Y.; Koch, H.; Kalugin, A.; Krylenko, I.; et al. An ensemble analysis of climate change impacts on streamflow seasonality across 11 large river basins. *Clim. Change* **2017**, *141*, 401–417. [[CrossRef](#)]
54. Sharmila, S.; Joseph, S.; Sahai, A.K.; Abhilash, S.; Chattopadhyay, R. Future Projection of Indian Summer Monsoon Variability under Climate Change Scenario: An Assessment from CMIP5 Climate Models. *Glob. Planet. Change* **2015**, *124*, 62–78. [[CrossRef](#)]
55. Kumar, D. River Ganges—historical, cultural and socioeconomic attributes. *Aquat. Ecosyst. Health Manag.* **2017**, *20*, 8–20. [[CrossRef](#)]
56. Byun, K.; Chiu, C.; Hamlet, A.F. Effects of 21st century climate change on seasonal flow regimes and hydrologic extremes over the Midwest and Great Lakes region of the US. *Sci. Total Environ.* **2019**, *650*, 1261–1277. [[CrossRef](#)]
57. Feng, D.; Beighley, E. Identifying uncertainties in hydrologic fluxes and seasonality from hydrologic model components for climate change impact assessments. *Hydrol. Earth Syst. Sci.* **2020**, *24*, 2253–2267. [[CrossRef](#)]
58. Garijo, C. Influence of climate change on flood magnitude and seasonality in the Arga River catchment in Spain. *Acta Geophys.* **2018**, *66*, 769–790. [[CrossRef](#)]
59. Dinpashoh, Y.; Singh, V.P.; Biazar, S.M.; Kavehkar, S. Impact of climate change on streamflow timing (case study: Guilan Province). *Theor. Appl. Climatol.* **2019**, *138*, 65–76. [[CrossRef](#)]
60. Kuriqi, A.; Ali, R.; Pham, Q.B.; Montenegro Gambini, J.; Gupta, V.; Malik, A.; Linh, N.T.T.; Joshi, Y.; Anh, D.T.; Nam, V.T.; et al. Seasonality shift and streamflow flow variability trends in central India. *Acta Geophys.* **2020**, *68*, 1461–1475. [[CrossRef](#)]
61. Mishra, V.; Shah, H.; López, M.R.R.; Lobanova, A.; Krysanova, V. Does comprehensive evaluation of hydrological models influence projected changes of mean and high flows in the Godavari River basin? *Clim. Change* **2020**, *163*, 1187–1205. [[CrossRef](#)]
62. Kundzewicz, Z.W.; Krysanova, V.; Benestad, R.E.; Hov, Ø.; Piniewski, M.; Otto, I.M. Uncertainty in climate change impacts on water resources. *Environ. Sci. Policy* **2018**, *79*, 1–8. [[CrossRef](#)]
63. Farinosi, F.; Arias, M.E.; Lee, E.; Longo, M.; Pereira, F.F.; Livino, A.; Moorcroft, P.R.; Briscoe, J. Future Climate and Land Use Change Impacts on River Flows in the Tapajós Basin in the Brazilian Amazon. *Earth's Futur.* **2019**, *7*, 993–1017. [[CrossRef](#)]
64. Mishra, V.; Lilhare, R. Hydrologic sensitivity of Indian sub-continental river basins to climate change. *Glob. Planet. Change* **2016**, *139*, 78–96. [[CrossRef](#)]
65. Mishra, V.; Kumar, R.; Shah, H.L.; Samaniego, L.; Eisner, S.; Yang, T. Multimodel assessment of sensitivity and uncertainty of evapotranspiration and a proxy for available water resources under climate change. *Clim. Change* **2017**, *141*, 451–465. [[CrossRef](#)]
66. Yang, T.; Cui, T.; Xu, C.Y.; Ciais, P.; Shi, P. Development of a new IHA method for impact assessment of climate change on flow regime. *Glob. Planet. Change* **2017**, *156*, 68–79. [[CrossRef](#)]
67. Yu, Z.; Gu, H.; Wang, J.; Xia, J.; Lu, B. Effect of projected climate change on the hydrological regime of the Yangtze River Basin, China. *Stoch. Environ. Res. Risk Assess.* **2018**, *32*, 1–16. [[CrossRef](#)]
68. Bajracharya, A.R.; Bajracharya, S.R.; Shrestha, A.B.; Maharjan, S.B. Climate change impact assessment on the hydrological regime of the Kaligandaki Basin, Nepal. *Sci. Total Environ.* **2018**, *625*, 837–848. [[CrossRef](#)]
69. Mcfarlane, D.; George, R.; Ruprecht, J.; Charles, S.; Hodgson, G. Runoff and groundwater responses to climate change in South West Australia. *J. R. Soc. West. Aust.* **2020**, *103*, 9–27.
70. Awotwi, A.; Anornu, G.K.; Quaye-Ballard, J.; Annor, T.; Forkuo, E.K. Analysis of climate and anthropogenic impacts on runoff in the Lower Pra River Basin of Ghana. *Heliyon* **2017**, *3*, e00477. [[CrossRef](#)]
71. He, X.; Wada, Y.; Wanders, N.; Sheffield, J. Intensification of hydrological drought in California by human water management. *Geophys. Res. Lett.* **2017**, *44*, 1777–1785. [[CrossRef](#)]
72. Fazel, N.; Haghighi, A.T.; Kløve, B. Analysis of land use and climate change impacts by comparing river flow records for headwaters and lowland reaches. *Glob. Planet. Change* **2017**, *158*, 47–56. [[CrossRef](#)]
73. Wang, X.; Yang, T.; Wortmann, M.; Shi, P.; Hattermann, F. Analysis of multi-dimensional hydrological alterations under climate change for four major river basins in different climate zones. *Clim. Change* **2017**, *141*, 483–498. [[CrossRef](#)]
74. Ashraf, S.; AghaKouchak, A.; Nazemi, A.; Mirchi, A.; Sadegh, M.; Mofatkhari, H.R.; Hassanzadeh, E.; Miao, C.Y.; Madani, K.; Mousavi Baygi, M.; et al. Compounding effects of human activities and climatic changes on surface water availability in Iran. *Clim. Change* **2019**, *152*, 379–391. [[CrossRef](#)]
75. Hattermann, F.F.; Vetter, T.; Breuer, L.; Su, B.; Daggupati, P.; Donnelly, C.; Fekete, B.; Florke, F.; Gosling, S.N.; Hoffmann, P.; et al. Sources of uncertainty in hydrological climate impact assessment: A cross-scale study. *Environ. Res. Lett.* **2018**, *13*, 015006. [[CrossRef](#)]
76. Ito, R.; Shiogama, H.; Nakaegawa, T.; Takayabu, I. Uncertainties in climate change projections covered by the ISIMIP and CORDEX model subsets from CMIP5. *Geosci. Model Dev.* **2020**, *13*, 859–872. [[CrossRef](#)]

77. McSweeney, C.F.; Jones, R.G. How representative is the spread of climate projections from the 5 CMIP5 GCMs used in ISI-MIP? *Clim. Serv.* **2016**, *1*, 24–29. [[CrossRef](#)]
78. Liu, X.; Tang, Q.; Cui, H.; Mu, M.; Gerten, D.; Gosling, S.N.; Masaki, Y.; Satoh, Y.; Wada, Y. Multimodel uncertainty changes in simulated river flows induced by human impact parameterizations. *Environ. Res. Lett.* **2017**, *12*, 025009. [[CrossRef](#)]
79. Krysanova, V.; Zaherpour, J.; Didovets, I.; Gosling, S.N.; Gerten, D.; Hanasaki, N.; Schmied, H.M.; Pokhrel, Y.; Satoh, Y.; Tang, Q.; et al. How evaluation of global hydrological models can help to improve credibility of river discharge projections under climate change. *Clim. Change* **2020**, *163*, 1353–1377. [[CrossRef](#)]